Accepted Manuscript: https://doi.org/10.1016/j.ijhydene.2019.05.028

H_2-based synthetic fuels: A techno-economic comparison of alcohol, ether and hydrocarbon production

Steffen Schemme,[a,b,*] Janos Lucian Breuer,[a] Maximilian Köller,[a] Sven Meschede,[a] Fiona Walman,[a] Remzi Can Samsun,[a] Ralf Peters[a] and Detlef Stolten[a,b,c]

[a] Electrochemical Process Engineering (IEK-3), Forschungszentrum Jülich GmbH, 52425, Jülich, Germany

[b] JARA-ENERGY, 52056 Aachen, Germany

[c] Chair for Fuel Cells, RWTH Aachen University, 52072, Aachen, Germany

*Corresponding author. Tel: +49 2461 61-2779; fax: +49 2461 61-6695; E-mail address: s.schemme@fz-juelich.de

Manuscript accepted for publication in *International Journal of Hydrogen Energy*.

- https://doi.org/10.1016/j.ijhydene.2019.05.028
- Received 15 February 2019
- Received in revised from 22 April 2019
- Accepted 3 May 2019

Keywords

- Power-to-Fuel
- Electrofuels
- Sector coupling
- DME
- OME_1, OME_{3-5}
- Fischer-Tropsch

Highlights

- Techno-economic analysis of Power-to-Fuel processes from a comparative perspective
- Chemical plant design in Aspen Plus® for Power-to-Fuel pathways
- All simulations with the same assumptions and under the same boundary conditions
- Flowsheet–based, component-specific cost calculation
- Production-specific advantages and disadvantages of various e-fuels

Abstract

Electricity-based fuels are one promising option to achieve the transition of the energy system, and especially the transport sector, in order to minimize the role of fossil energy carriers. One major problem is the lacking compatibility between different techno-economic assessments, such that recommendations regarding the most promising Power-to-Fuel technology are difficult to make. This work provides a technically sound comparison of various Power-to-Fuel options regarding technological maturity and efficiency, as well as cost. The investigated options include methanol, ethanol, butanol, octanol, DME, OME_{3-5} and hydrocarbons. To guarantee the comparability, all necessary chemical plants were designed in Aspen Plus® to determine material and energy consumption, as well as investment costs within the same boundary conditions and assumptions in all simulations and calculations. Individual technical aspects of the various synthesis routes, as well as their advantages and disadvantages, are highlighted.

With an assumed electrolysis efficiency of 70% and considering the energy demand for the CO_2 supply and the energy and operating material demand of the chemical plants, depending on the selected electrofuel, 30–60% of the primary energy in renewable electricity can be stored in the lower heating value of the electrofuel. In the presented results, the costs of H_2 supply are responsible for 58–83% of the total manufacturing costs and thus have the greatest potential to reduce the latter. For the base case (4.6 €/kg_{H2}), various electrofuels will have costs of manufacturing of between 1.85–3.96 €/l_{DE}, with DME being the cheapest.

1. Introduction

To limit anthropogenic climate change [1], a holistic transformation of the energy system that minimizes the role of fossil energy carriers is essential, which also requires a transformation of the transportation sector [2]. As stated by several studies [3-9] and position statements [10-14], Power-to-Fuel (also known as Power-to-Liquid/PTL) technologies are indispensable for achieving a largely greenhouse gas-neutral energy supply in the future. This is particularly the case for air, shipping and heavy goods traffic [15, 16]. In the PTL concept, regeneratively-generated electricity is used to produce hydrogen (H_2) via water electrolysis. Then, H_2 and CO_2 are used in a chemical process to synthesize fuels. These fuels are often called electrofuels [17]. Conversion to other chemicals is also possible, which allows coupling between the energy and chemical sectors. The required CO_2 can, for instance, be sequestrated from industrial exhaust gases or ambient air. Although the production costs of electric fuels are currently well above the market prices of conventional fuels [18], they have the potential to compete with conventional fuels [5, 16, 19].

The use of electrofuels promotes the development and expansion of hydrogen technologies while simultaneously using the existing fuel infrastructure and vehicles. With the PTL concept, the secondary energy carrier H_2 can be used in all parts of the transport sector with comparatively little effort. The high energy demand of the entire transport sector creates promising storage possibilities for the fluctuating energy supply from renewable sources. As with all H_2 technologies, this paves the way for the expansion of renewable energy generation. Amongst others, due to omitting market entry barriers, electrofuels are ideal for supplementing electro mobility with H_2/fuel cells and batteries, as well as biofuels. As discussed by Schemme et al. [20], such a diversification will be needed in the future, as is the case with today's available fuels and mobility technologies.

As pointed out by Bongartz et al. [21], on the one hand, the direct use of H_2 in fuel cell vehicles has better well-to-wheel efficiencies, higher greenhouse gas reduction potential in relation to conventional

fuels, lower emissions and lower fuel costs compared to the use of electrofuels. On the other hand, fuel cell vehicles have higher costs due to their recent market introduction; in addition, the necessary infrastructure requires corresponding investment.

Various technologies are currently under discussion for the technical implementation of the power-to-fuel concept. Especially alcohols, ethers and hydrocarbons are of great interest for the use as fuels [20]. Schemme et al. [22] developed new H_2-based synthesis routes for higher alcohol synthesis by adapting known and novel chemical processes and assessing the technical maturity via TRL. The synthesis routes towards higher ethers published by Burger [23] are suitable for the power-to-fuel concept since they all start with the intermediate product methanol.

Brynolf et al. [24] published a literature review of calculated production costs of electric fuels in early 2017, finding the following number of sources per electric fuel: 12 x CH_4, 5 x methanol, 2 x DME, 6 x Fischer-Tropsch (FT), 2 x Methanol-to-Gasoline (MTG) . Additionally to the literature reviewed by Brynolf et al. [24], recently, H_2-based OME_{3-5} synthesis routes has been analyzed in terms of energy efficiency [25]. However, it is not clear how technically mature, efficient and expensive different PTL technologies are, as the comparability of different publications is not guaranteed due to the varying choice of assumptions and methodologies. The problem of the unguaranteed compatibility is clearly evident in the works of Haarlemmer et al. [26] and Brynolf et al. [24] in the comparison of techno-economic analyses of various working groups with regard to coal, natural gas and biomass or electricity-based fuel synthesis. Thus, one important message from Haarlemmer et al. [26] is that the interpretation of a single calculation may lead to false inferences due to the influence of the assumptions.

The scientific contribution of this work is a simulation-based techno-economic analysis and a comparative assessment of the necessary process steps for the production of promising electrofuels. Additionally, the technical maturity is compared via the technology readiness level (TRL) [27, 28]. The uniqueness of the presented work is that all process simulations and calculations are carried out under identical boundary conditions and with the same assumptions.

2. Selection of Electrofuels

For the comparison, the following electrofuels are selected:

- Methanol in accordance with IMPCA [29], permitted by EN 228 [30]
- Ethanol in accordance with EN 15376 [31] (USA: ASTM 4806), permitted by EN 228 [30]
- 1-Butanol in accordance with ASTM D7862 [32], permitted by EN 228 [30]
- 2-Butanol in accordance with ASTM D7862 [32], permitted by EN 228 [30]
- iso-Octanol (no standard available)
- DME in accordance with ISO 16861 [33]
- OME_1 (no standard available)
- OME_{3-5} in accordance with DIN 51699 (proposal) [34]
- Synthetic gasoline in accordance with EN 228 [30]
- Paraffinic diesel in accordance with EN 15940 [35]
- Paraffinic kerosene (FT-SPK) in accordance with ASTM D7566 [36]

DME and OME_n are abbreviations for dimethyl ether and polyoxy dimethyl ether. As stated by Schemme et al. [22], methanol, ethanol, 1-butanol and 2-butanol, as well as 1-octanol, are promising alcohols for fuel use. However, for 1-octanol, no suitable synthesis route based on H_2 and CO_2 has yet been identified. Therefore, in this work, iso-octanol, instead of 1-octanol, was selected for comparison, as their physical properties are very similar.

Figure 1 shows the synthesis routes selected for comparison. The selection of the synthesis routes towards higher alcohols to compare is illustrated in Figure 1 and in accord with the work of Schemme et al. [22], whereby only synthesis route with process steps with TRL ≥ 4 were selected. Therefore, the process steps for butanol and octanol are based on the aldol condensation. TRL ≥ 4 means that it is validated at least at the laboratory scale.

For DME synthesis, the state-of-the-art synthesis via methanol was selected (see Figure 1). The selected synthesis routes, A, B and C, towards OME_{3-5} illustrated in Figure 1 are derived from Burger [23] with the variation that with Formalin I and Formalin II, aqueous and methanol-containing formaldehyde solutions with different methanol contents are used. As it is the case for the alcohol synthesis routes, all required process steps for the OME_{3-5} synthesis routes have TRL ≥ 4 (see Supplementary Material). In case synthesis gas is required (see Figure 1), a reverse water-gas shift (RWGS) reactor is used. This technology has a TRL of 6 [37]. For the synthesis of paraffinic diesel and kerosene, the Fischer-Tropsch (FT) process is selected, as this process is industrially in use and special fuel standards exist (EN 15940 [35] and the ASTM D7566 (FT-SPK) [36]).

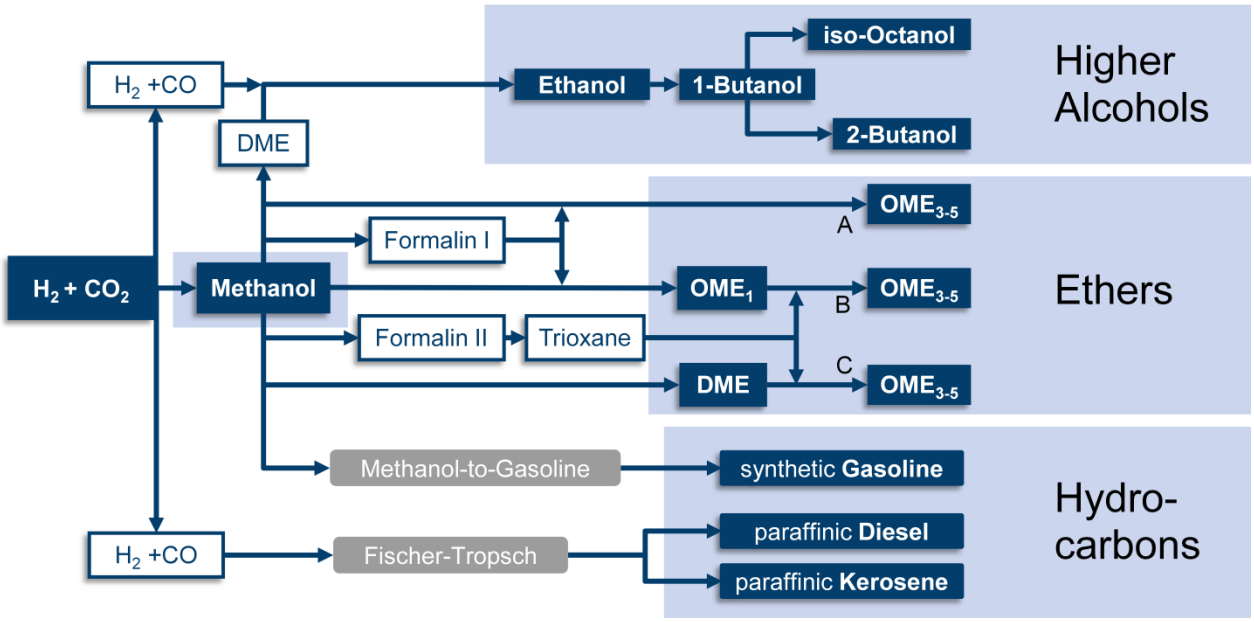

Figure 1. Selected synthesis routes for comparative assessment.

3. Methodology

To ensure comparability in a techno-economic analysis, uniform system boundaries, a uniform methodology and the use of identical assumptions are fundamental. To simplify the integration of the results into system analytical investigations, the system boundary was chosen to be as small as possible. This work does not explicitly distinguish between central and decentralized plants, as this is only relevant at a system analytical level. The educt supply of water electrolysis and CO_2 sequestration is not part of the analysis framework. By decoupling H_2 production from the chemical plant, the system framework is compatible with pipeline-based energy systems that aim to supply H_2 to the road transport sector, such as those developed by Seydel [38] and Krieg [39]. These concepts of a complete H_2 infrastructure include production from wind power, compression, storage in salt caverns, and distribution. Within these energy concepts, flexibly operable PEM electrolyzers are to be used that already have a comparatively high degree of technological maturity (TRL). This also allows the chemical plant to run continuously without

any major temporary storage, which makes the entire system more flexible. In a study published by LBST in 2016, full market penetration of PEM electrolysis is expected by 2040 [40]. A successful large-scale market entry would be supported by automated and standardized production, which is especially true for PEM electrolysis [41]. PEM electrolysis has been extensively reviewed by Carmo et al. [42].

For practical and efficient simulations, the sub-processes of the synthesis routes are not simulated in a coherent way, but rather individually and then reassembled into synthesis routes according to a modular principle. With the help of the process simulations, the raw material and utility demand for each modular sub-process are determined in a standardized manner on the respective product. The raw material and energy consumption of a synthesis route or production chain results from the material and energy balancing based on the mass and energy balances arising from the individual sub-processes. When handing over an intermediate product stream across the system boundary of a sub-process, pressure and temperature levels, as well as compositions, are maintained, and mass balances complied. The precise pressures and temperatures depend on the process on the one hand and on the material properties, such as melting and boiling points, on the other. The impurities of the intermediates are neglected, so that at the interfaces, material streams with a purity of 100% are handed over to the next module. Therefore, for intermediates, a purity of at least 99 wt.-% is ensured. The calculated efficiency and costs for the H_2-based production of a specific fuel includes the energy demand and cost for all process steps towards intermediates on the synthesis route.

3.1. Assumptions and boundary conditions

For an overview, reproducibility and traceability, important assumptions made in the context of this work and the boundary conditions are listed in Table 1. Discussion regarding the assumptions can be found in the Supplementary Material. The target products of the simulated processes are fuels in accordance with the corresponding fuel standard (see Section 2).

A plant size of 300 MW fuel output based on the lower heating value is a realistic capacity. It is in the upper capacity range of decentralized biofuel production plants [43] and a global average cement plant emits enough CO_2 to cover the raw material demand of a 300 MW synthesis plant (see Supplementary Material). The values of the energy demand and the cost for CO_2 supply listed in Table 1 are not correlated. The value for the energy demand is used to calculate the Power-to-Fuel efficiency (Eq. 5). The value for the CO_2 cost is used in the economic analysis. The H_2 price of 4.6 €/kg is based on a scenario analysis of a complete H_2 infrastructure (including fluctuating production from wind power, compression, storage in salt caverns and a pipeline system) for the transport sector, minus the costs for refueling stations and the distribution network [44]. A complete nationwide H_2 infrastructure ensures a continuous H_2 supply and thus enables the chemical plants to operate continuously.

Table 1. Assumptions and boundary conditions.

Parameter	Value	Reference / Notes
Efficiency of PEM electrolysis based on LHV	0.7	[45-47]
Energy expenditure of CO_2 sequestration	1.2 MJ_{el}/kg_{CO2}	[48], see Supp. Material
CO_2 feed conditions	25 °C 30 bar	- [49]
H_2 feed conditions	25 °C 30 bar	- [50, 51]
Temperature change of cooling water	20-25 °C	-
Temperature change of cooling air	30-35 °C	-
High pressure (HP) saturated steam Medium pressure (MP) process steam Low pressure (LP) process steam	250 °C, 39.7 bar 175 °C, 8.9 bar 125°C, 2.3 bar	-
Isentropic efficiency of compressors	76%	[52, 53]
Efficiency of pumps	60%	[52, 53 (p. 762)]
Maximum compression ratio per stage	3	-
Minimum temperature difference	10 K	-
Pressure losses	-	-
Cost of H_2	4.6 €/kg_{H2}	according to [44]
Cost of CO_2	70 €/t_{CO2}	[24]
Cost of saturated steam	32 €/t	[54]
Cost of high-pressure steam (250 °C)	0.0187 €/MJ	calculated from 32 €/t
Cost of medium-pressure steam (175 °C)	0.0158 €/MJ	
Cost of low-pressure steam (125 °C)	0.0146 €/MJ	
Cost of operating electricity	0.0976 €/kWh	[55]
Cost of cooling water	0.1 €/t	[54]
Cost of cooling air	0	-
Plant size	≈ 300 MW	-
Lifespan of the plants	20 year	[3, 56-58]
Interest rate	8%	[57]
Currency conversion	US$/€ = 1.21	[59]
Operating hours per year	8000 h/a	-
Depreciation method	Annuity	-
Lower heating value of diesel (LHV)	35.9 MJ/l	[60 (p. 13)]

3.2. Utilities and processing mediums

Various utilities and processing media are required for the operation of chemical plants. Similar to a composite site (*in German: Verbundstandort*) [61] within the simulations, saturated steam (also: process steam) at different temperature levels provides external process heat. This is particularly necessary for distillative separations, but is also used in other process operations, such as the regeneration of molecular sieves. In this work, the availability of saturated steam at three different pressure levels, which are common in the chemical processing industry, is assumed (see Table 1). The saturated steam can be

used for heating as well as cooling operations and serves as a heat transfer medium. Due to the choice of three different pressure levels, the use of waste heat at lower temperatures and a more cost-effective heat supply are possible. In addition, the heat integration of several sub-processes of a synthesis can be more flexibly and efficiently implemented in this way.
Considering a minimum temperature difference of 10 K, cooling water allows a process stream to be cooled to 30 °C. Process operations, which operate at a lower temperature, must be cooled with coolants. Coolants are not provided externally, but cooling is instead carried out locally in the plant by compression refrigerators.
The energy demand for cooling is determined by the operational power required for the compressor of the compression refrigerator. High pressure steam is not hot enough to provide heat at temperatures > 240 °C. Therefore, if heat cannot be internally provided in a process, electrical heating or firing is necessary.

3.3. Process optimization

In PTL processes, the cost for H_2 makes up by far the highest share of production costs. The adapted and developed processes are therefore first optimized in terms of conversion and yield. The next optimization step is local heat integration within the respective sub-processes. This step is taken directly, using heat exchanger networks, as well as indirectly with the help of saturated steam. The supply and withdrawal of the required and excess steam from sub-processes across their system boundaries enables the global heat integration of the respective synthesis routes. This minimizes the intra-route heat demand by using waste heat from individual sub-processes. At this point it should be noted that a heat integration bound to process steam pressure levels differs from the commonly used ideal heat integration via pinch-analysis. The strict compliance with the use of specified utilities can lead to a higher heat demand compared to the ideal heat integration. However, it is closer to the technical implementation.

3.4. Process efficiencies

Unlike most chemical processes, either the raw materials and products are energy carriers, or their provision can be presented in the form of energy expenditure in the processes analyzed and assessed in this work. Additionally, all processing mediums can be indicated in terms of energy demand. This allows for a straightforward calculation of efficiencies. The efficiency of each synthesis route is evaluated using the energetic efficiency according to equations 2 to 5. These are common definitions in the literature [18, 25, 57, 62-65].

Electrolysis efficiency (system efficiency based on the LHV):
$$\boldsymbol{\eta_{H2}} = \frac{\dot{m}_{H2} \cdot LHV_{H2}}{P_{electrolysis}} \quad \text{Eq. 1}$$

Chemical conversion efficiency:
$$\boldsymbol{\eta_{LHV}} = \frac{\dot{m}_{Fuel} \cdot LHV_{Fuel}}{\dot{m}_{H2} \cdot LHV_{H2}} \quad \text{Eq. 2}$$

Plant efficiency:
$$\boldsymbol{\eta_{Plant}} = \frac{\dot{m}_{Fuel} \cdot LHV_{Fuel}}{\dot{m}_{H2} \cdot LHV_{H2} + P_{Plant}} \quad \text{Eq. 3}$$

Efficiency factor:
$$\boldsymbol{f} = \frac{\eta_{Plant}}{\eta_{LHV}} \quad \text{Eq. 4}$$

Power-to-Fuel efficiency:
$$\boldsymbol{\eta_{PTL}} = \frac{\dot{m}_{Fuel} \cdot LHV_{Fuel}}{\frac{\dot{m}_{H2} \cdot LHV_{H2}}{\eta_{H2}} + P_{CO2} + P_{Plant}} \quad \text{Eq. 5}$$

3.5. Fuel equivalent

The fuel equivalent is used for energy standardization, as the different electrofuels have different heating values. Thus, the specific cost and energy demand can be compared, for instance. The energy content of conventional fuels is not clearly defined and is based on the composition. In this work, we use the values published by the Joint Research Centre (JRC: CONCAWE, EUCAR, European Commission): LHV_{Diesel} = 35.9 MJ/l (43.1 MJ/kg) and $LHV_{Gasoline}$ = 32.2 MJ/l (43.2 MJ/kg) [60 (p. 13)]. The energy content of 1 kg H_2 with 119.96 MJ/kg [66] corresponds to the energy content of 3.34 liters of conventional petroleum-based diesel fuel or 3.73 liters of conventional petroleum-based gasoline. Diesel equivalent (DE) is used for comparability, as most of the electrofuels investigated in this work are suitable for diesel engines. To calculate the values in relation to the gasoline equivalents, the respective values must be multiplied by 1.115 (35.9/32.2).

3.6. Economic analysis and evaluation

The costs of manufacturing (COM) are estimated on the basis of the total capital requirements and operating costs. The capital-related costs are included in the production costs as an imputed depreciation, as well as interest. Except for the costs for raw materials and processing mediums, all operational expenditures (OPEX) depend on the investment costs [67-69]. The fixed capital investment (FCI) for the simulated chemical plants are estimated by means of the component-specific cost calculation method developed by Turton et al. [68]. The authors give a detailed breakdown of the derivation of specific apparatus costs up to the final investment amount.

The direct and fixed manufacturing costs and the general expenses, which are based on the FCI, are also calculated in accordance with Turton et al. [68] using the proposed average values. To determine personnel costs, the method discussed by Alkhayat and Gerrard [70] is used. A working capital of 15% of the FCI is assumed. Personnel costs are part of the direct OPEX and determined by the number of unit operations.

The component cost approach for estimating the FCI is a recognized method that is frequently used in scientific and feasibility studies. According to the definitions of AACE International [71], the estimation accuracy of this approach is -30% to +50%. Using component-specific rather than global surcharge factors, the estimation accuracy can vary in direction by -15% to +20%.

The component sizing is based on the flowsheet calculations in Aspen Plus®. The dimensioning of the components considers a minimum and a maximum component size. For example, if a distillation column with a diameter of 12 m is theoretically required to ensure the desired throughput, nine columns are used instead due to the maximum diameter value of 4 m.

4. Simulations

In the following, the different sub-processes for the synthesis routes shown in Figure 1 are briefly described. Linking the sub-processes leads to cost and energy demand of whole synthesis routes. All the sub-processes are simulated using the process simulation software, Aspen Plus®, for the steady state. Additional information on the modeling of RWGS reactors as well as flowsheets, reaction equations, energy balances, product quality, and important aspects of the processes described in the following are given in the Supplementary Material.

4.1. Methanol from H_2 and CO_2

The process developed in the course of this work for the synthesis of methanol from H_2 and CO_2 is based on the process concept proposed by Otto [72]. Hansen and Nielsen [73] report that commercial copper

catalysts achieve high selectivities of 99.9% and that the use of CO_2 instead of CO further reduces the amount of by-products. Therefore, by-products are neglected and only one distillation column is needed for the treatment of the raw methanol. Thus, the product purification is similar to the process concepts described in the literature [21, 72, 74-76]. No external heat supply is required for the operation of such plants, as the heat demand can be met internally by making use of the reactor's waste heat. Real plants for the synthesis of methanol from synthesis gas have two or three distillation columns for product treatment due to possible by-products. According to the process simulation, the product purity is 99.9 wt.-%.

4.2. DME from Methanol

The simulation model was designed on the basis of the processes proposed by Inclusive Science Engineering [77] and Otto [72] and optimized by customized pressures in the columns, as well as improved heat integration. Referring to Müller and Hübsch [78], the selectivity for the DME synthesis via methanol dehydration is close to 100%. By-products are therefore neglected in the simulation. The mixing gap of the ternary component system methanol / water / DME is bypassed. The product achieves the desired DME purity of > 99.9 wt.-% for intermediates. At the same time, containing the requirements for DME as a fuel according to ISO 16861 [33] are fulfilled.

4.3. Ethanol from DME, H_2 and CO_2

The raw materials for the ethanol synthesis are DME and synthesis gas. The required synthesis gas is provided via a RWGS reactor from H_2 and CO_2. Due to thermodynamic factors, the use of the RWGS reactor leads to residues of CO_2 and CH_4 in the synthesis gas. The influence of methane on ethanol synthesis is neglected in this work due to the data situation, while methane is considered as an inert component in the ethanol reactor. In the ethanol reactor, CO and DME are first converted into methyl acetate through carbonylation. Methyl acetate is then hydrated to methanol and ethanol. Possible by-products of this reaction are CO_2 and ethyl acetate [79, 80]. Even without water, the present component system has four binary azeotropes: methanol / methyl acetate, methanol / ethyl acetate, ethanol / ethyl acetate and DME / ethanol. For process-analytical modelling, the thermodynamic model used determines these azeotropes with sufficient accuracy. For example, the composition and temperature of the azeotrope ethanol / ethyl acetate is determined with a deviation of < 4% and < 1%, respectively, from the measurement data of Pavlicek et al. [81]. In addition to the azeotropes, another aspect is that the boiling points of ethanol and ethyl acetate, as well as those of methanol and methyl acetate, are close together. Both aspects represent a challenge for distillative treatment. Due to recycling streams and the integration of a reformer operated with oxygen to convert non-recyclable by-products, no by-products other than water leave the process. With a purity of 98.7 wt.-%, ethanol and the other shares, the product corresponds to EN 15376 [31] for fuel ethanol.

4.4. 1-Butanol from Ethanol

This process was developed for the first time in the course of this work, using the reaction kinetics developed by Riittonen et al. [82]. In addition to 1-butanol, the by-products of acetaldehyde, ethyl acetate and diethyl ether are also formed from ethanol due to the aldol condensation of ethanol in the reactor [82]. Furthermore, ethanol reacts with the by-product acetaldehyde to 1,1-diethoxy ethane. The reactions take place in the liquid phase. The by-products, which cannot be recycled back into the reactor, are reformed using oxygen and water and used as raw materials for the methanol synthesis. This must be taken into account when linking the sub-processes to a synthesis route. With 99.9 wt.-%, the purity of

1-butanol exceeds, for instance, the value of 99.8 wt.-% in the safety data sheet for 1-butanol of the Carl Roth GmbH + Co KG [83].

4.5. 2-Butanol from 1-Butanol

According to the process concept developed in this work, 1-butanol is first dehydrated to butene. The corresponding reactor is designed on the basis of the investigations carried out by Khan et al. [84]. To provide the heat, an H_2 burner is used to avoid CO_2 emissions. In a subsequent reactor, butene is hydrated to 2-butanol. The technical implementation can be carried out, for instance, by the strong-acid process [85]. Here, instead of indirect hydration, direct hydration is assumed. For the chosen reaction conditions, the thermodynamic equilibrium is entirely on the product side, resulting in 100% conversion and selectivity.

4.6. Iso-Octanol from 1-Butanol

This process concept for the synthesis of iso-octanol (1- ethyl hexanol) was first developed in the course of this work and is based on the aldol condensation starting from 1-butanol. As it has the potential, according to Patankar and Yadav [86], to reduce manufacturing costs compared to the industrial standard synthesis with two reaction steps, in this work the direct synthesis is simulated. The reactor design for the dehydration of 1-butanol to butanal is based on the studies of Raizada et al. [87]. The required supply of heat at high temperatures is covered using an H_2 burner to avoid CO_2 emissions. In the next step, butanal is converted by the aldol condensation into the unsaturated aldehyde iso-octenal (2-ethyl-2-hexenal) and then hydrated into iso-octanol. According to the simulation, the iso-octanol produced within the developed process has a purity of 99.7 wt.-% (99.7 mol.-%).

4.7. Formaldehyde from Methanol

The process concept for the formaldehyde synthesis is based on the catalytic oxidation of methanol with partial methanol conversion of the chemical company ICI (Imperial Chemical Industries), whose technical implementation was described by Reuss et al [88] and Chauvel and Levebre [89].

To enable the thermodynamic modelling of the aqueous and methanol-containing formaldehyde solutions, a UNIFAC-based reaction model based on the work of Maurer [90] and Albert et al. [91] is implemented. The missing component data of hemiformals, methylene glycols and OME_n with $n > 1$, are partly estimated using data from the literature and predicted using the Aspen Plus® Property Constant Estimation System. The implemented model considers the strongly non-ideal thermodynamic behavior due to the constantly reacting component equilibrium, even outside the reaction zones of the simulation model. The implemented model is validated using binary and ternary phase diagrams, as well as the concentration and temperature profiles of the distillation columns. The reactor is modeled using an Aspen Plus® RPlug reactor model in which the kinetic published by Panzer and Emig [92] is implemented.

Special features of the designed processes are the process variations for the synthesis of formaldehyde solutions with different compositions (see Figure 1: formalin I and formalin II; see Supplementary Material). Thereby, in the case of the synthesis of formalin I, the process economy was improved compared to the standard process design. In addition, the absorber unit was optimized by integrating waste water streams from other sub-processes of the OME_{3-5} synthesis routes B and C.

4.8. Trioxane from Formalin

For the synthesis of trioxane from formalin, the process developed by Grützner [93] is simulated, optimized and analyzed. The technical feasibility of the process concept proposed by Grützner [93] has been demonstrated both in simulations and in laboratory experiments and studies on pilot plants are

currently being planned [94]. In addition, the purification process by means of pressure swing rectification is patented [95]. The technical maturity of the process is estimated to be TRL 5.
To increase the separation effect, the interconnection of the columns was changed and the number of theoretical separation stages of some columns specified by Grützner [93] was slightly increased. The reflux ratios of the distillation columns have also been adjusted. Furthermore, the pressures of individual columns were increased to enable heat recovery via steam generation in the condensers. As a result, 47% of the required heat can be recovered in the form of low-pressure steam through steam generation. Despite the further optimization of Grützner's already innovative distillative process [93], the trioxane synthesis is a highly energy-intensive process. In addition to the large recycle streams resulting from the unfavorable equilibrium of the reaction, the high energy demand due to large distillate streams should be noted. The product purity of trioxane is 99.98 wt.-%.

4.9. OME_1 from Formalin and Methanol

The synthesis of OME_1 (methylal) was designed in accordance with the patented concept [96] described by Drunsel [97]. The TRL of this process concept is estimated at TRL of minimum 5. The reaction is modeld using the activity coefficient based kinetic model published by Drunsel [97].
Due to the azeotropic component system methanol / OME_1, a pressure swing distillation is used. In the simulation, the formaldehyde content of < 1 wt.-% in the reactor product and the associated oligomerization reactions are considered. Thanks to this detailed simulation, an optimization option for the process to produce formalin I in the upstream of the OME_1 synthesis has been identified. The product has a purity of 99.9 wt.-% OME_1. In the context of process interconnection, a special feature of this work is that bottom streams that contain only water and low shares of formaldehyde are used as absorbents in the formalin synthesis.

4.10. OME_{3-5} via synthesis route A

The simulated process concept for the synthesis of OME_{3-5} from methanol and formalin is based on the concept published by Schmitz et al. [98] and patented by the OME Technologies GmbH [99]. The technical maturity of this process concept is estimated to be TRL of minimum 4.The product composition of the reactor was modeled with the substance quantity based equilibrium constants published by Oestreich et al. [100]. In the process concept of Schmitz et al. [98], the reactor requires a feed with a water content of 0–0.2 wt.-%. However, formaldehyde synthesis through the oxy dehydration of methanol delivers an aqueous formaldehyde solution with equal molar shares of formaldehyde and water. To ensure the correct interconnection of both synthesis plants, the concept published by Schmitz et al. [98] was modified to consider purification of the formaldehyde. Additionally, the process concept was arranged with the available utilities (process steam at three different pressure levels). The special features of the process developed and simulated in the course of this work are the installation of molecular sieves between the reactant compression and the reactor and between the reactor and the pressure swing distillation, improved heat integration and a modified arrangement of distillation columns and recycle streams. The product purity is 99 wt.-%. The product composition is given in the Supplementary Material.

4.11. OME_{3-5} via synthesis route B

The process concept for the OME_{3-5} synthesis from trioxane and OME_1 simulated in this work is proposed by Burger et al. [101]. The technical maturity is assessed with TRL of minimum 4. As the component system of OME_n, trioxane and formaldehyde does not contain water or methanol, no oligomerization reactions of formalin take place. The energy required for operating the vacuum distillation is also

considered in the energy balance. The product purity is 99 wt.-%. The product composition is given in the Supplementary Material.

4.12. OME_{3-5} via synthesis route C

The process concept for the OME_{3-5} synthesis from DME and trioxane is based on the process concept for the OME_{3-5} synthesis from OME_1 and trioxane. Since the synthesis was validated on laboratory scale, the TRL is estimated to be 4. For the simulation, the reaction mechanism is described by pseudo-equilibrium constants which are determined based on the work of Haltenort et al. [102]. The simulated process concept is a best case, as the separation in the distillation columns tends to be more complex due to the occurrence of unforeseen thermodynamic effects. The product purity is 99 wt.-%. The product composition is given in the Supplementary Material.

4.13. Hydrocarbons via Methanol-to-Gasoline Process

Target product of the MTG-process is synthetic gasoline which is in accordance with the conventional standard EN 228 [30]. In the designed process concept, the methanol synthesis from H_2 and CO_2 and the MTG process are directly linked. The MTG reactor is assumed to be an innovative fluidized bed reactor. This technology is industrially demonstrated [103]. The product distribution of the MTG-reactor is derived from the work of Phillips et al. [104]. Special feature of the process concept is that light gases which do not correspond to the gasoline fraction are reformed using pure O_2 and H_2O. The reformer is operated auto thermal and the product distribution is determined by calculating the minimum Gibbs free energy using the Aspen Plus® *RGibbs* reactor model. The outlet temperature of the reformer is controlled by the O_2 supply and set to be 900 °C to ensure the technical feasibility with regard to adiabatic combustion temperatures in the oxidation zone of the reformer. The generated synthesis gas is fed to the methanol reactor. Thereby, the process has no by-products except water and the only product is synthetic gasoline. Further information on the process concept and regarding the product quality can be found in the Supplementary Material.

4.14. Hydrocarbons via Fischer-Tropsch Process

The simulated process consists of a RWGS reactor, a reformer, a Fischer-Tropsch (FT) reactor, a hydrocracker and a distillation column. In the distillation column, steam is used as an entrainer. Referring to de Klerk [105, 106] and Dry [107], for low temperature FT synthesis using cobalt catalysts, only unbranched alkanes with the molecular formula of C_nH_{2n+2} are considered. The product distribution is determined using the Anderson-Flory-Schulz (ASF) approach [108, 109]. The chain growth probability is described using the model of Vervloet et al. [110]. C_{30+} hydrocarbons are split into three groups of pseudo-components: C_{30}-C_{35}, C_{36}-C_{47} und C_{48+}. The average molecule of the C_{48+} component group is $C_{61}H_{124}$. The supply of synthesis gas for the FT reactor is covered by the RWGS reactor and the reformer. In particular, the use of the reformer to recycle C-fractions, which are too short to be assigned to the kerosene fraction, is a unique aspect of the overall process. In the reformer, these C-fractions are converted into synthesis gas using O_2 and H_2O. The recycling of short hydrocarbons separated by stepwise cooling from the FT product stream to the RWGS reactor is typical for low temperature FT synthesis with cobalt catalysts [111]. In the developed process, these gases are partly directed to the reformer, which relieves the electric preheating of the input stream of the RWGS reactor. The developed process has no CO_2 emissions, does not require an external heat supply and the only products are paraffinic diesel, paraffinic kerosene and the water by-product. The products meet the requirements of the fuel standards EN 15940 [35] and ASTM D7566 (FT-SPK), respectively [36] (see Supplementary Material).

5. Results and Discussion

Figure 2 shows the comparison of the energy demand as well as the Power-to-Fuel η_{PTL} and chemical conversion efficiencies η_{LHV} of the various synthesis routes towards alcohols, ethers and hydrocarbons based on H_2 and CO_2 presented in Figure 1. The values shown in Figure 2 are listed in the Supplementary Material. The energy demand presented is the energetic equivalent of one liter of diesel, the values being independent of the size of the plant.

The dotted connecting lines of the displayed efficiencies of η_{PTL} and η_{LHV} in Figure 2 serve to improve orientation. For H_2, η_{LHV} is 1 and η_{PTL} is equal to the electrolysis efficiency of 0.7. Figure 2 also shows the energy surpluses of saturated steam and the heat to be discharged by cooling water as a negative energy demand. This surplus saturated steam can be used, for instance, to cover or reduce the heat demand of raw material supply concerning electrolysis or CO_2 sequestration. In the case of the CO_2 sequestration, this would reduce or eliminate the red bars in Figure 2 and thus increase the Power-to-Fuel efficiency η_{PTL}. With 4.66 MJ_{Steam}/kg_{CO2} medium-pressure steam and 1.91 MJ_{Steam}/kg_{CO2} low-pressure steam, the FT process has a total surplus heat of 6.57 MJ_{Steam}/kg_{CO2}. This is, for example, in the range of heat demand of 5.4–7.2 MJ/kg_{CO2} (at 95 °C) [16, 40] of the adsorption/desorption process for carbon capture from the ambient air of Climeworks AG. In case the energy demand for the CO_2 supply in the Power-to-Fuel efficiency η_{PTL} (Eq. *5*) is set to zero due to the use of surplus heat for CO_2 sequestration, the FT synthesis' efficiency (η_{PTL}) would increase from 50.6% to 52.8% and the red bar of FT in Figure 2 would disappear. Thus, FT plants are suitable for operation even without an industrial CO_2 point source supplying enough heat for CO_2 sequestration from ambient air. This is a particular advantage for the FT process. Another option for use of the surplus heat is to provide steam for high temperature electrolysis, which allows an η_{PTL} of up to 70%, as demonstrated by sunfire GmbH [112].

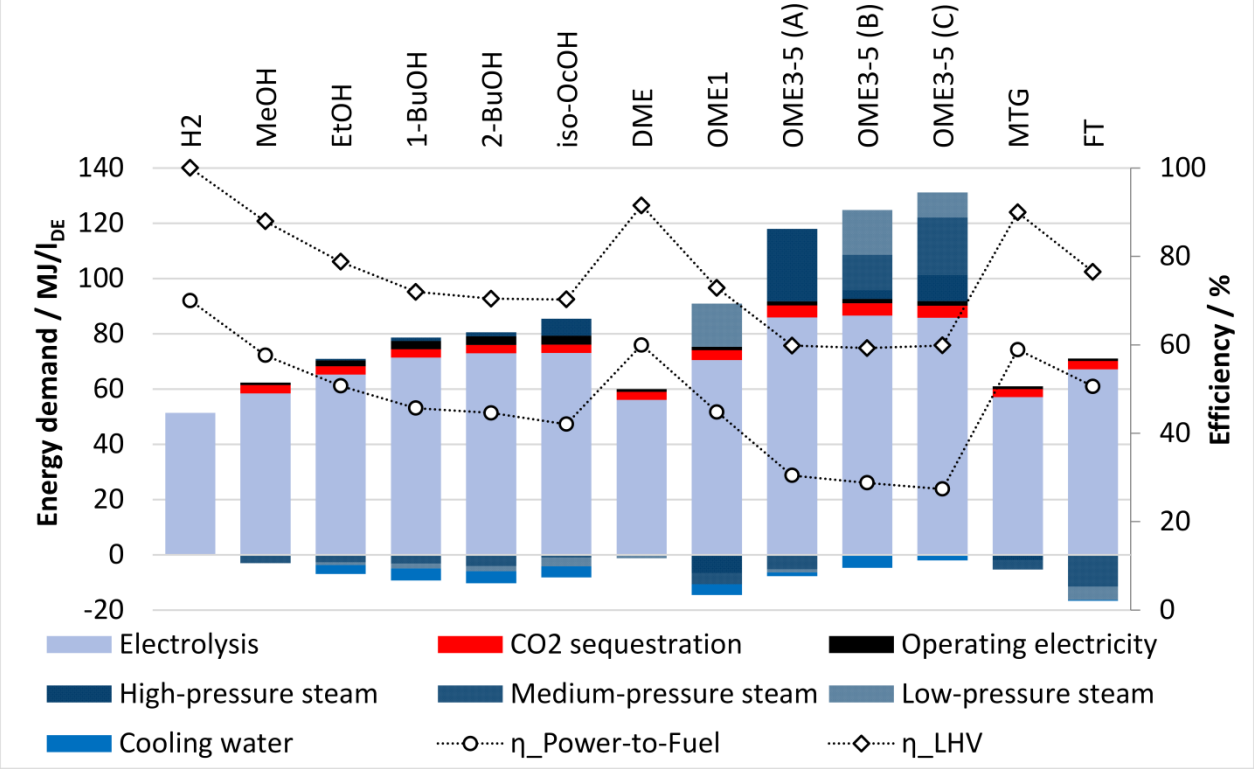

Figure 2. Comparison of the energy demand for the synthesis of 1 l_{DE} electrofuel.

Figure 2 also illustrates the increasing energy demand along the synthesis routes to higher alcohols. The biggest drop in efficiency is due to the synthesis step from methanol to ethanol. The reason for this is, amongst others, the necessary use of a RWGS reactor with the preheating input stream for the synthesis gas supply from H_2 and CO_2, as well as the reformer for the recycling of not directly recyclable by-products. The reformer used in the 1-butanol synthesis from ethanol to recover by-products also leads to higher H_2 demand.

In the FT process, 53.0 wt.-% of the water-free reactor product is passed to the reformer. In the MTG process, this amount is only 18.8 wt.-%. The reformer of the FT process has a O_2 demand of 0.386 $kg_{O2}/kg_{FT\ products}$ (0.315 kg_{O2}/l_{DE}). In the MTG process, in contrast, the reformer requires 0.134 $kg_{O2}/kg_{MTG\ product}$ (0.111 kg_{O2}/l_{DE}). Since the O_2 must be sequestrated from the process due to formation of water, the increased O_2 demand of the FT process also increases the demand of H2, as shown clearly in Figure 2 and Table A1.

Although DME is a follow-up product of methanol, DME has, with 60%, the highest Power-to-Fuel efficiency η_{PTL}. This is mainly because methanol is liquid and DME is gaseous under standard conditions. A further explanation and a plausibility test regarding the efficiencies is given in the Supplementary Material. As listed in

Table A2 in the Appendix and illustrated in Figure 2, the amount of excess heat in the form of process steam is lower in the synthesis of DME in MJ/l_{DE} as well as in MJ/kg_{CO2}. The reason for this is that steam produced via the waste heat from the methanol reactor is used to cover the heat demand of the product treatment in the DME synthesis. As a result, the potential to reduce the energy demand of the CO_2 sequestration (red bars in Figure 2) is lower for DME production than for methanol production.

In OME_1 production based on H_2 and CO_2, a Power-to-Fuel efficiency of η_{PTL} = 0.448 is achieved on the condition that the formaldehyde-containing waste water of the OME_1 synthesis plant is used as an absorbent in the upstream synthesis of formalin I. Using pure water instead of waste water as an absorbent results in η_{PTL} = 0.443. By using the waste water, the H_2 demand drops from 0.275 kg/kg_{OME1} to 0.270 kg/kg_{OME1} while the CO_2 demand drops from 3.039 kg/l_{DE} to 2.987 kg/l_{DE}. The H_2 demand for OME_1 production is significantly lower than for $OME_{3\text{-}5}$ production, because less formaldehyde is needed per l_{DE}.

The relatively low maximum chemical conversion efficiencies $\eta_{LHV,max}$ (see

Table A2 in the Appendix) show a non-influenceable limitation of the $OME_{3\text{-}5}$ synthesis. Due to the complex separation processes for water separation, the plant efficiency η_{Plant} (Eq. 3) is also low, which is also reflected in the comparatively low efficiency factors of the $OME_{3\text{-}5}$ synthesis routes. As is shown in Figure 2, the most energetically advantageous $OME_{3\text{-}5}$ synthesis route is synthesis route A. However, $OME_{3\text{-}5}$ synthesis via route A requires high pressure steam.

Heat surplus in the form of saturated steam at a higher temperature level can be used to cover the demand for steam at a lower temperature level. This is performed with the synthesis route to OME_1, which reduces the low pressure steam demand from 15.6 MJ/l_{DE} auf 5.0 MJ/l_{DE}. The process no longer has a surplus of high and medium pressure steam, as is shown in Figure 2. Without this internal heat recovery, the plant efficiency η_{Plant} would not be 0.543, instead of 0.643 (η_{PTL} drops from 0.448 to 0.401).

For the sake of completeness, the specific raw material demands of H_2 and CO_2, the surplus heat in the form of saturated steam after intra-route heat integration, as well as the technology readiness level (TRL) as an indicator of the technical maturity, and finally the efficiencies of all synthesis routes, according to equations 2 to 5, are given in Table A1 and

Table A2 in the Appendix.

Figure 3 shows the comparison of the specific shares of the costs of manufacturing of the various electrofuels in the base case. The values shown in Figure 3 are listed in the Supplementary Material. The value of 1.38 €/l_{DE} for H_2 given in Figure 3 represents the cost of 4.6 €/kg_{H2} (see Table 1). This value is added to the figure to present the starting point.

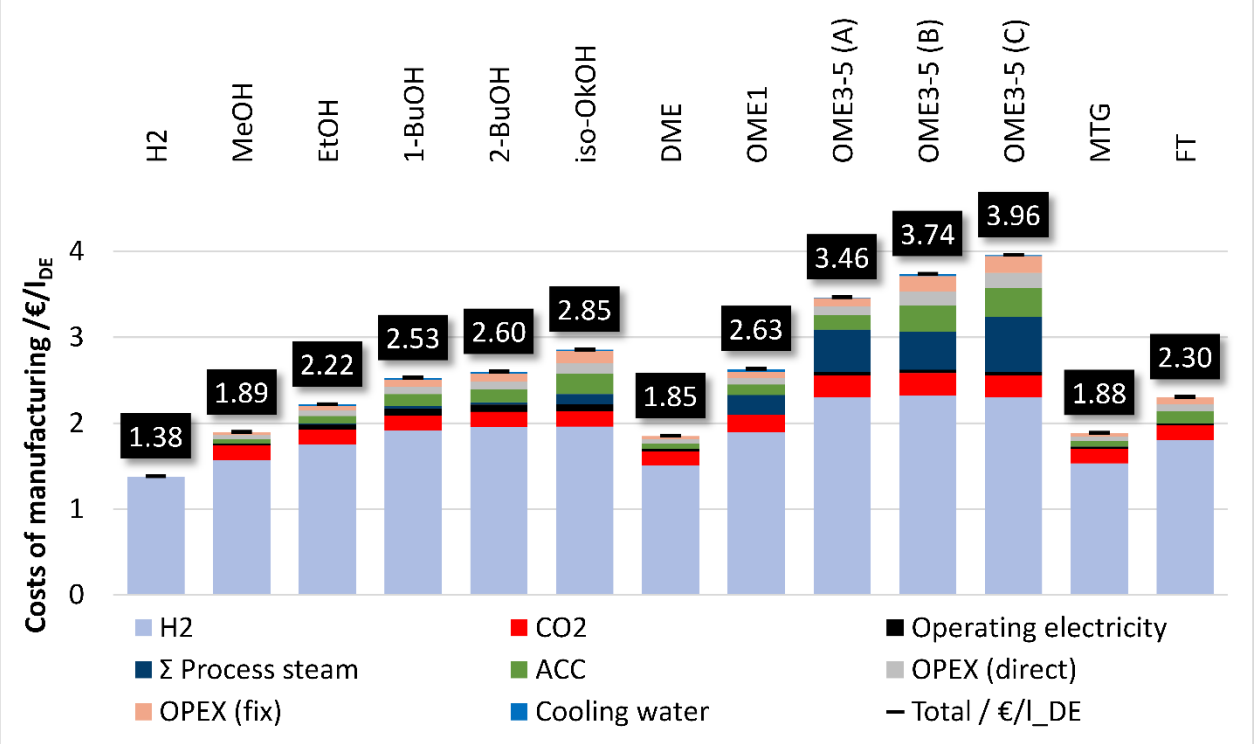

Figure 3. Comparison of base case costs for the synthesis of 1 l_{DE} electrofuel.

Referring to the energy content, DME and methanol exhibit the lowest costs of manufacturing, with 1.85 €/l_{DE} and 1.89 €/l_{DE}, respectively. Mass based, the costs of manufacturing for methanol and DME are 1.05 €/kg and DME 1.49 €/kg, respectively. That, referring to the energy content, a follow-up product can be less cost intensive than the intermediates product is also the case for MTG products.

These are followed by ethanol and Fischer-Tropsch fuels, with 2.22 €/l_{DE} and 2.30 €/l_{DE}. 1- and 2-butanol, with 2.53 €/l_{DE} and 2.60 €/l_{DE}, have similar costs to OME_1 with 2.63 €/l_{DE}. The remarkably high demand of processing mediums in the form of saturated steam in the OME_{3-5} synthesis in Figure 2 also has a significant impact on the costs of manufacturing, as Figure 3 illustrates. The cost share of operating electricity is relatively small. As illustrated in Figure 3, the specific cost for the process steam in €/l_{DE} for the OME_{3-5} synthesis via route A are higher than those for OME_{3-5} synthesis via route B, even though the specific energy demand in MJ/l_{DE} is lower, as is shown in Figure 2. This is due to the different cost for the process steam at different temperature levels (see Table 1). The comparison of the cost components in Figure 3 shows the impact of required investment costs (ACC), which entail further costs caused by OPEX, such as maintenance, insurance and tax.

Sensitivity analyses are carried out to assess the sensitivity of the calculated values. The varied parameters are listed in Table 2. The FCI are varied within the range of the estimation accuracy as per AACE International. According to Machhammer et al. [113], H_2 produced via electrolysis using wind and grid power without grid charges costs, on average, 6 €/kg and 3 €/kg, respectively. These two values are used to vary the H_2 costs. For the costs of the CO_2 supply, the minimum value given by Brynolf et al. [24]

is used for CO_2 capture from exhaust gas from natural gas power plants (0.02 €/kg_{CO2}) and the maximum value for capture from exhaust gases from coal-fired power plants (0.17 €/kg_{CO2}). The costs for cooling water and process steam are varied between +/-50%. The limits of the costs of operating electricity come from the BDEW electricity price analysis from 2016 for large industrial customers [55]. It should be noted here that, in accordance with the method of Turton et al. [68], the variations in raw material and operating medium costs, as well as investment costs, have an impact on the OPEX and thus an additional indirect impact on the costs of manufacturing.

Table 2. Upper and lower bound of parameters for the sensitivity analysis.

	Unit	Lower bound	Base case	Upper bound
Cost of H_2	€/kg	3	4.6	6
Cost of CO_2	€/kg	0.02	0.07	0.17
CAPEX	-	-30%	-	+50%
Interest rate	-	2%	8%	12%
Process steam	€/t	16	32	48
Cooling water	€/t	-50%	0,1	+50%
Operating electricity	€ct/kWh	4	9.76	14.7

Of the eleven compared synthesis routes, two representative synthesis routes are used at this point for the sensitivity analysis in the form of tornado diagrams. These are the synthesis routes with the lowest and highest share of H_2 costs as part of the manufacturing costs: OME_{3-5} via route C, with 58.1%, and methanol, with 82.8%.

Figure 4 and Figure 5 illustrate the corresponding sensitivity analysis results using values listed in Table 2. For the simpler comparison, the intervals of the y-axes are identical. In case only the lower or upper limits of the parameters listed in Table 2 are used for calculating the costs of manufacturing, the cost range for methanol is 1.15–2.71 €/l_{DE} and for OME_{3-5} (C), 2.28–5.91 €/l_{DE}.

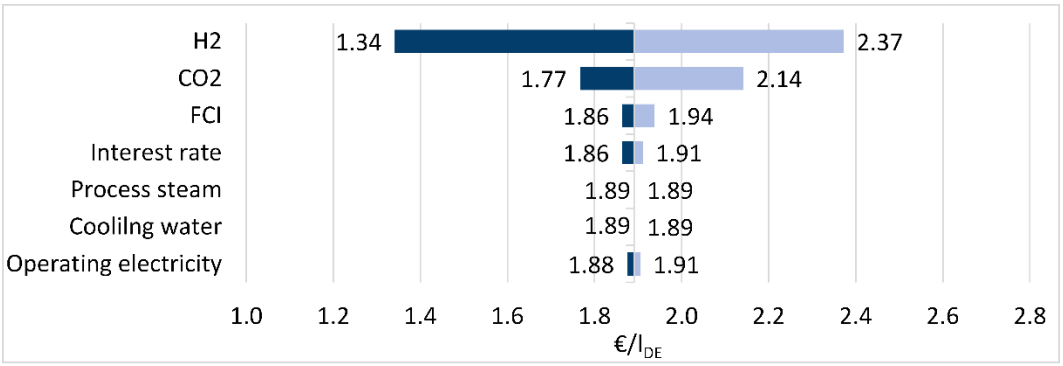

Figure 4. Sensitivity analysis regarding the synthesis costs of methanol from H_2 and CO_2

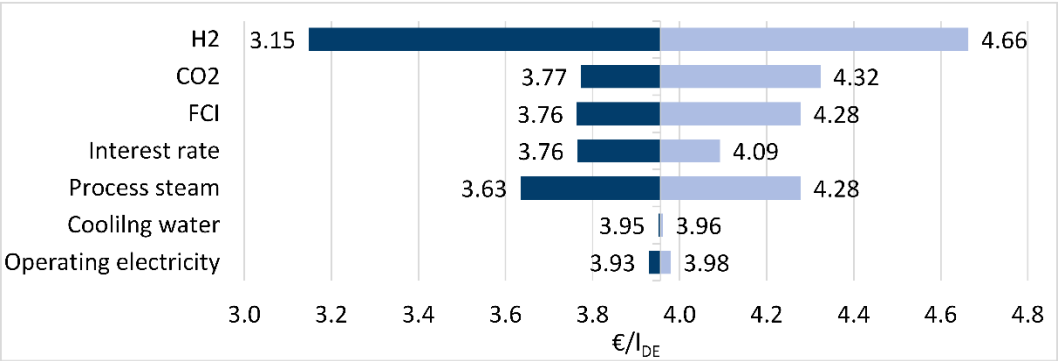

Figure 5. Sensitivity analysis regarding the synthesis costs of OME_{3-5} via route C from H_2 and CO_2.

Due to the low or non-existent demand for process mediums, the variation in the associated costs has almost no influence on the methanol process. With specific investment costs of 235.4 €/kW, the plant is also significantly cheaper than those required for the OME_{3-5} synthesis via route C with 1625.5 €/kW. Amongst other reasons, this is because of the significantly different FCI, ACC and OPEX accounting for 6.6% of the manufacturing costs in the methanol base case and 17.9% in the OME_{3-5} (C) base case. The influence of the FCI estimation accuracy and interest rate varies accordingly. The costs of manufacturing of OME_{3-5} (C) are more sensitive to the H_2 costs. This is due to the O_2 input for oxy dehydration in the formalin synthesis, which leads to additional H_2O generation, resulting in increased H_2 demand. Figure 5 shows that the cost of manufacturing of OME_{3-5} via synthesis route C from H_2 and CO_2 are also sensitive to the cost of process steam, which in the base case accounts for 16.1%. If there is a lot of waste heat at the production site, for example due to a steel mill process, it could be utilized wisely to supply the OME_{3-5} production. Further sensitivity analysis results regarding the synthesis of the remaining electrofuels shown in Figure 3 can be found in the appendix.
Overall, the production of OME_{3-5} from H_2 and CO_2 is significantly more energy- and cost-intensive than the production of alcohols, DME and hydrocarbons. For a deeper overview, the production of the various electrofuels is discussed and evaluated separately below.

Methanol and DME

The processes for synthesizing methanol and DME are less complex and more technically mature compared to other processes studied in this work. The production of DME from methanol is also state-of-the-art and widely used. If, in contrast to the usual technical application, the methanol process is driven with only one column, as is often suggested in the literature, no external heat supply is required. By-products are also not a challenge to the already highly developed catalysts. It should be noted that using reactor models that predict product distributions based on thermodynamic equilibrium is an estimation of the best case potential.

Ethanol

The developed process concept for the synthesis of ethanol is based on laboratory results from the literature and therefore has a TRL of 4. Although Mixed-Alcohol-Synthesis is an already technically realized process, it has insufficient selectivity for large-scale production. One challenge is the product separation, as by-products and intermediates in the reactor product lead to a mixture with several binary azeotropes. In the process developed in the course of this work, the high reactor pressure of 140 bar, as well as the use of a RWGS reactor whose feed gases must be electrically preheated, the compression refrigerator and reformer for the utilization of non-recyclable by-products lead to an increased need for electrical energy and H_2 input. If the kinetics were known, it could be investigated whether an adapted

reactor control would decrease the share of by-products. Therefore, at this point, the process concept seems to have an optimization potential.

Butanol

As is shown in Figure 2 and Figure 3, the specific H_2 demand increases when moving from ethanol to 1-butanol, although ethanol is the only raw material in the 1-butanol synthesis. The increase in H_2 demand is also reflected in the chemical conversion efficiency η_{LHV}, which decreases from ethanol to 1-butanol by almost 6.8 percentage points, although the $\eta_{LHV,max}$ only decreases by 1.7 percentage points (see

Table A2 in the Appendix). The reason for this is the use of a reformer for the recovery of by-products and the associated O_2 feed into the system, which must be separated by water formation. The synthesis gas obtained by reforming by-products can be fed into the ethanol synthesis. This has a positive impact on the efficiency of the synthesis route. Although no by-products are produced in the process of synthesizing 2-butanol from 1-butanol, the H_2 demand increases. This is due to the required H_2 burner to provide heat at high temperatures. An electric heater could also be used at this point. However, the technical feasibility could not be assessed in the context of this work. The H_2 demand of the burner increases the H_2 costs by 0.042 €/l_{DE}.

Octanol

As with the process concept to convert 1-butanol to 2-butanol, the process concept of iso-octanol synthesis requires an H_2 burner for the heat required by the dehydration of 1-butanol to butanal. When comparing the bars of 1-butanol and iso-octanol in Figure 3, there is an increased demand for process steam and higher annual capital costs (ACC). The main reason for this is the highly energy- and cost-intensive product treatment. The azeotropic reactor product contains 36 mol.-% iso-octanol in the thermodynamic equilibrium. Iso-octanol has the highest boiling point of the mixture and is therefore subtracted through the bottom stream of the distillation column. Amongst the five sub-processes for the synthesis of iso-octanol, the last plant on the route is responsible for 40.3% of the investment costs. The distillation column to separate the iso-octanol is responsible for 18.2% of the total investment costs of the whole synthesis route.

OME_{3-5}

The sub-processes of the OME_{3-5} synthesis routes known from the literature have been adapted and further developed. These adjustments include, for example, the use of three process variants in formaldehyde synthesis, in particular the saving of the separation column of the formaldehyde process for route A. Thus, subsequent sub-processes can be provided with an increased surplus of process steam and investment costs can be saved. A second example is the improved heat recovery by steam generation in the condensers of the distillation columns of the trioxane process. A third example is the optimization of the OME_{3-5} synthesis from methanol and formalin known from the literature. An alternative arrangement of adsorber beds for water separation reduces the loading of the distillation columns and, additionally, shifts the chemical equilibrium in the reactor towards the products. Overall, the OME_{3-5} synthesis routes are already highly optimized from a process engineering point of view and a decisive potential for further energy savings is not currently apparent to the authors of this work.

Figure 2 shows that the sole process analysis does not yet show which of the three OME_{3-5} synthesis routes is preferable. In accordance with the lower process steam demand, the plant efficiency η_A (Eq. 3) of the synthesis via route A is three percentage points higher than for route B (see

Table A2 in the Appendix) and more than five percentage points higher than for route C. It should be noted here that the calculations of the efficiencies do not consider the different pressure levels of the saturated steam. These generate different energy-related costs (base case: 32 €/t_{steam}) and temperature and pressure-dependent enthalpy of evaporation. The costs for process steam for production via synthesis route A in the base case is 0.489 €/l_{DE}. For route B, the cost is lower (0.439 €/l_{DE}) and for route C higher (0.637 €/l_{DE}). As is shown in Figure 3, the economically-preferable OME_{3-5} synthesis route is route A. The main reasons for this include the significantly higher capital-related and operating costs of routes B and C, mainly caused by the sub-process of trioxane synthesis.

Hydrocarbons

H_2-based hydrocarbon syntheses via Fischer-Tropsch (FT) and Methanol-to-Gasoline (MTG) have a high technological maturity of TRL 6 and TRL 9, respectively. In both processes, short hydrocarbons are produced in the synthesis reactor, which do not correspond to the fractions of the desired products. These are reformed under O_2 and H_2O intake. The fed-in O_2 is removed from the process by water formation and separation. This results in an increased H_2 demand. For this reason, as few hydrocarbons as possible should be reformed. As the formation reactions are chain growth reactions, the reactor control also affects the product distribution. Since the amount of short hydrocarbons which needs to be reformed is significantly larger in the FT process, the H_2 demand of the FT process is significantly higher than the H_2 demand of the combined methanol and MTG process.

In the FT process, there is further H_2 saving potential through improved process arrangement and control. Overall, the process has a lot of adjustment options whose effects are influenced by each other, which makes process optimization highly complex. By increasing the size of the plant, there is further potential to save investment costs.

The comparison in Table 3 serves to answer the central research question of this work, namely how technically mature, energy- and cost-intensive Power-to-Fuel processes are compared to one another. The values result from the techno-economic analysis. MP and LP are abbreviations for medium pressure and low pressure steam (see Table 1). The CAPEX values refer to the LHV of the fuel output.

Table 3. Overview of key values and results of the techno-economic assessment of different electrofuels.

	Methanol	Ethanol	1-Butanol	2-Butanol	iso-Octanol	DME	OME_1	OME_{3-5} (Route A)	synth. Gasoline (MTG)	synth. Diesel (FT)	synth. Kerosene (FT)
TRL	9	4	4	4	4	9 (SoA)	5	4	9 (SoA)	6 (SoA)	
LHV / MJ/kg	19.92	26.76	33.10	33.00	37.56	28.83	19.92	19.22	43,5	43.9	44.2
€/l_{DE}	1.891	2.216	2.527	2.599	2.859	1.849	2.628	3.463	1.883	2.303	
CAPEX / €/kW	235.4	557.9	673.0	728.8	1137.3	297.9	577.9	793.9	312.5	666.6	
Excess heat / MJ/kg_{CO2}	1.21 (MP) 0.07 (LP)	0.99 (MP) 0.39 (LP)	1.23 (MP) 0.71 (LP)	1.62 (MP) 0.78 (LP)	0.45 (MP) 1.23 (LP)	0.04 (MP) 0.37 (LP)	-	1.30 (MP) 0.34 (LP)	0.85 (HP) 1.35 (MP) 0.11 (LP)	4.66 (MP) 1.91 (LP)	
kg_{H2}/l_{DE}	0.340	0.380	0.416	0.425	0.426	0.327	0.270	0.500	0.333	0.391	
η_{LHV} (Eq. 2)	0.880	0.788	0.720	0.704	0.702	0.916	0.729	0.598	0.899	0.765	
η_A (Eq. 3)	0.859	0.744	0.662	0.612	0.593	0.894	0.643	0.409	0.875	0.749	
η_{PTL} (Eq. 5)	0.576	0.507	0.457	0.438	0.420	0.600	0.448	0.305	0.589	0.506	
Available standard specification	IMPCA, AA-Grade	EN 15376	ASTM D7862	ASTM D7862	-	ISO 16861	-	(DIN 51699)	EN 228	EN 15940	ASTM D7566

6. Conclusion

All products of the simulated processes meet the requirements of the corresponding fuel specifications or, in case of OME_{3-5}, of a proposal for a fuel specification. The comparability of the synthesis processes is fully guaranteed, as all simulations and calculations have been carried out with identical assumptions and boundary conditions.

The Power-to-Fuel technologies that are techno-economically compared in this work already have a high technological maturity (TRL 9 or at least TRL ≥ 4) and the production of high-quality synthetic fuels is technically feasible. Assuming an electrolysis efficiency of $70\%_{LHV}$, a Power-to-Fuel efficiency of 30–60% can be achieved to produce the different electrofuels studied. This already includes the electrolysis efficiency. Accordingly, depending on the selected electrofuel, 30–60% of the primary energy in electricity can be stored in the lower heating value of the electrofuel. In the presented cases, the costs of H_2 supply are responsible for 58–83% of the total manufacturing costs, depending on the electrofuel and synthesis route. H_2 supply is, accordingly, the main cost driver and thus has the greatest potential to reduce the cost of manufacturing of the electrofuels. For the base case (4.6 €/kg_{H2}), the various electrofuels will have costs of manufacturing between 1.85–3.96 €/l_{DE}, with DME being the cheapest and OME_{3-5} produced via synthesis route C the most expensive electrofuel.

Compared to the other options, the syntheses of methanol and DME have the highest technical maturity, the highest Power-to-Fuel efficiencies and the lowest manufacturing costs. The selective synthesis of higher alcohols based on H_2 and CO_2 is technically feasible. The main challenges are the formation of by-products and low technical maturity. Further catalyst improvements are needed to enhance the process efficiency and decrease the costs of manufacturing. The production of OME_{3-5} from H_2 and CO_2 is significantly more energy- and cost-intensive than the production of alcohols, DME and hydrocarbons. For the OME_{3-5} synthesis, route A is the most preferable in terms of energy and cost efficiency.

The MTG synthesis with combined with methanol synthesis from H_2 and CO_2 and a reformer to recycle light gases has been found as an efficient to produce H_2-based gasoline. The adaption and process optimization of the Fischer-Tropsch process, which is already well-established in terms of technology, has promising future applicability as it is the only method for producing jet fuel based on H_2 and CO_2 with high technical maturity. Improved process arrangements and reactor control strategies can enhance the synthesis. In particular, the Fischer-Tropsch process is well suited to an interconnection with CO_2 sequestration from ambient air, as the corresponding heat demand can be covered through the reactor waste heat.

7. Abbreviations and Subscripts

AACE	Association for the Advancement of Cost Engineering
ACC	Annual capital costs
BuOH	Butanol
CAPEX	Capital expenditures
DE	Diesel equivalent
DME	Dimethyl ethers
e-fuel	Electrofuel
EtOH	Ethanol
FCI	Fixed capital investment
FT	Fischer-Tropsch
GE	Gasoline equivalent

HP	High pressure steam
LHV	Lower heating value
LP	Low pressure steam
max	Maximum possible
MeOH	Methanol
MP	Medium pressure steam
OcOH	Octanol
OME_n	Polyoxymethylene dimethyl ethers
OPEX	Operational expenditures
PEM	Polymer electrolyte membrane
PTL	Power-to-Liquid
RWGS	Reverse water-gas shift
SM	Supplementary Material
TRL	Technology Readiness Level
η_{PTL}	Power-to-Fuel efficiency
η_{Plant}	Plant efficiency
η_{LHV}	Chemical conversion efficiency

Acknowledgements

The authors would like to thank Joachim Pasel, Maximilian Decker, Stefan Weiske – all based at the Forschungszentrum Jülich GmbH, Institute of Energy and Climate Research, IEK-3 – Electrochemical Process Engineering – for their valuable input. Further thanks are addressed to the members of the JARA Energy seed fund, "Power to Fuel," and its successor – The Competence Center Power to Fuel. JARA (Jülich-Aachen Research Alliance) is an initiative of RWTH Aachen University and the Forschungszentrum Jülich. Additionally, this work was partly performed within the framework of the project house TESYS (Technology-based energy systems analysis) of RWTH Aachen University, financed by the Excellence Initiative of the German federal and state governments to promote science and research at German universities.

References

1. IPCC, *Climate Change 2013: The Physical Science Basis. Contribution of Working Group I to the Fifth Assessment Report of the Intergovernmental Panel on Climate Changer*. 2018, IPCC. p. 1585
2. Canzler, W., and Wittowsky, D., *The impact of Germany's Energiewende on the transport sector – Unsolved problems and conflicts.* Utilities Policy, 2016. **41**: p. 246-251 DOI: 10.1016/j.jup.2016.02.011.
3. Kramer, U., *Defossilierung des Transportsektors - Optionen und Voraussetzungen*. 2018
4. prognos, *Status und Perspektiven Flüssiger Energieträger in der Energiewende (Endbericht)*. 2018
5. Agora, *Agora Verkehrswende, Agora Energiewende und Frontier Economics - Die zukünftigen Kosten strombasierter synthetischer Kraftstoffe*. 2018
6. Gerbert, P., Herhold, P., Buchardt, J., Schöneberger, S., Rechenmacher, F., Kirchner, A., Kemmler, A., and Wünsch, M., *Klimapfade für Deutschland*. 2018, The Boston Consulting Group (BCG) und Prognos im Auftrag des Bundesverbandes der Deutschen Industrie (BDI)
7. Bründlinger, T., König, J. E., Frank, O., Gründig, D., Jugel, C., Kraft, P., Krieger, O., Mischinger, S., Prein, P., Seidl, H., Siegemund, S., Stolte, C., Teichmann, M., Willke, J., and Wolke, M., *dena Leitstudie Integrierte Energiewende - Impulste für die Gestaltung des Energiesystems bis 2050 (Ergebnisbericht und Handlungsempfehlungen)* 2018

8. Adolf, J., Balzer, C., Haase, F., Lenz, B., Lischke, A., and Knitschky, G., *SHELL Nutzfahrzeug-Studie: Diesel oder alternative Antriebe: Womit fahren Lkw und Bus morgen? - Fakten, Trends und Perspektiven bis 2040*. 2016
9. Purr, K., Osiek, D., Lange, M., Adlunger, K., Burger, A., Hain, B., Kuhnhenn, K., Lehmann, H., Mönch, L., Müschen, K., Proske, C., Schmied, M., and Vollmer, C., *Integration von Power to Gas/Power to Liquid in den laufenden Transformationsprozess*. 2016, Umweltbundesamt
10. Wagemann, K., and Ausfelder, F., *E-Fuels - Mehr als Option*. 2017, DECHEMA Gesellschaft für Chemische Technik und Biotechnologie e.V.: Frankfurt
11. Searle, S., and Christensen, A., *White Paper - Decarbonization Potential of Electrofuels in the European Union*. 2018, ICCT - International Council on Clean Transportation
12. DECHEMA, *Fortschrittliche alternative flüssige Brenn- und Kraftstoffe: Für Klimaschutz im globalen Rohstoffwandel - Positionspapier des ProcessNet-Arbeitsausschusses „Alternative flüssige und gasförmige Kraft- und Brennstoffe“*. 2017
13. BDI, *Positionspapier der deutschen Industrie zum Aufbau von Rahmenbedingungen für die e-fuels-Technologien "e-fuels - jetzt handeln und Chancen nutzen"*. 2018, Bundesverband der Deutschen Industrie e.V.
14. BMVBS, *Die Mobilitäts- und Kraftstoffstrategie der Bundesregierung (MKS) - Energie auf neuen Wegen*. 2013
15. Arnold, K., Kobiela, G., and Pastowski, A., *Technologiebericht 4.3 Power-to-liquids/-chemicals innerhalb des Forschungsprojekts TF_Energiewende*, in *Technologien für die Energiewende*. 2018
16. dena, *"e-fuel" study - The potential of electricity-based fuels for low-emission transport in the EU*. 2017
17. Ridjan, I., Mathiesen, B. V., and Connolly, D., *Terminology used for renewable liquid and gaseous fuels based on the conversion of electricity: a review.* Journal of Cleaner Production, 2016. **112, Part 5**: p. 3709-3720 DOI: 10.1016/j.jclepro.2015.05.117.
18. Tremel, A., Wasserscheid, P., Baldauf, M., and Hammer, T., *Techno-economic analysis for the synthesis of liquid and gaseous fuels based on hydrogen production via electrolysis.* International Journal of Hydrogen Energy, 2015. **40**(35): p. 11457–11464 DOI: 10.1016/j.ijhydene.2015.01.097.
19. Larsson, M., Grönkvist, S., and Alvfors, P., *Synthetic Fuels from Electricity for the Swedish Transport Sector: Comparison of Well to Wheel Energy Efficiencies and Costs.* Energy Procedia, 2015. **75**: p. 1875–1880 DOI: 10.1016/j.egypro.2015.07.169.
20. Schemme, S., Samsun, R. C., Peters, R., and Stolten, D., *Power-to-fuel as a key to sustainable transport systems – An analysis of diesel fuels produced from CO2 and renewable electricity.* Fuel, 2017. **205**: p. 198-221 DOI: 10.1016/j.fuel.2017.05.061.
21. Bongartz, D., Doré, L., Eichler, K., Grube, T., Heuser, B., Hombach, L. E., Robinius, M., Pischinger, S., Stolten, D., Walther, G., and Mitsos, A., *Comparison of light-duty transportation fuels produced from renewable hydrogen and green carbon dioxide.* Applied Energy, 2018. **231**: p. 757-767 DOI: doi.org/10.1016/j.apenergy.2018.09.106.
22. Schemme, S., Breuer, J. L., Samsun, R. C., Peters, R., and Stolten, D., *Promising catalytic synthesis pathways towards higher alcohols as suitable transport fuels based on H2 and CO2.* Journal of CO2 Utilization, 2018. **27**: p. 223-237 DOI: doi.org/10.1016/j.jcou.2018.07.013.
23. Burger, J., *A novel process for the production of diesel fuel additives by hierarchical design*, in *Scientific report series / Laboratory of Engineering Thermodynamics*. 2012, Techn. Univ: Kaiserslautern. p. 115
24. Brynolf, S., Taljegard, M., Grahn, M., and Hansson, J., *Electrofuels for the transport sector: A review of production costs.* Renewable and Sustainable Energy Reviews, 2018. **81**: p. 1887-1905 DOI: 10.1016/j.rser.2017.05.288.

25. Held, M., Tönges, Y., Pélerin, D., Härtl, M., Wachtmeister, G., and Burger, J., *On the energetic efficiency of producing polyoxymethylene dimethyl ethers from CO2 using electrical energy.* Energy & Environmental Science, 2019 DOI: 10.1039/C8EE02849D.
26. Haarlemmer, G., Boissonnet, G., Peduzzi, E., and Setier, P.-A., *Investment and production costs of synthetic fuels – A literature survey.* Energy, 2014. **66**: p. 667-676 DOI: 10.1016/j.energy.2014.01.093.
27. EC, *European Commission - Horizon 2020: Work Programme 2016-2017, 20. General Annexes: G. Technology readiness level (TRL).* 2017
28. EC, *European Commission - Technology Readiness Level Guidance Principles for Renewable Energy technologies - Final Report*. 2017: Brussels
29. IMPCA, *Methanol Reference Specification*. 2015, International Methanol Producers & Consumers Association: Brüssel
30. DIN, *DIN EN 228:2014-10 - Automotive fuels - Unleaded petrol - Requirements and test methods; German version EN 228:2012*. 2014
31. DIN, *EN 15376 Automotive fuels - Ethanol as a blending component for petrol - Requirements and test methods; German version*. 2014
32. ASTM, *Standard Specification for Butanol for Blending with Gasoline for Use as Automotive Spark-Ignition Engine Fuel*. 2017, ASTM International: West Conshohocken, PA DOI: 10.1520/D7862-17.
33. ISO, *ISO 16861:2015, Petroleum products - Fuels (class F) - Specification of dimethyl ether (DME)*. 2015. p. 5
34. Wilharm, T., and Stein, H. *OME as a Diesel Fuel: The way to a fuel specification*. in *Perspectives on Power-to-Liquids and Power-to-Chemicals 2018*. 2018. Freiburg.
35. DIN, *EN 15940:2016 - Kraftstoffe für Kraftfahrzeuge - Paraffinischer Dieselkraftstoff aus Synthese oder Hydrierungsverfahren - Anforderungen und Prüfverfahren; Deutsche Fassung* 2016
36. ASTM, *D7566-16b, Standard Specification for Aviation Turbine Fuel Containing Synthesized Hydrocarbons*. 2016, ASTM International: West Conshohocken, PA. p. 34 DOI: 10.1520/D7566-18.
37. Schmidt, P., Weindorf, W., Roth, A., Batteiger, V., and Riegel, F., *Power-to-Liquids - Potentials and Perspectives for the Future Supply of Renewable Aviation Fuel*. 2016, German Environment Agency
38. Seydel, P., *Entwicklung und Bewertung einer langfristigen regionalen Strategie zum Aufbau einer Wasserstoffinfrastruktur - auf Basis der Modellverknüpfung eines Geografischen Informationssystems und eines Energiesystemmodells*. 2008, ETH Zürich
39. Krieg, D., *Konzept und Kosten eines Pipelinesystems zur Versorgung des deutschen Straßenverkehrs mit Wasserstoff*. 2012, RWTH Aachen University
40. LBST, *Ludwig Bölkow Systemtechnik - Research Association for Combustion Engines - Renewables in Transport 2050 - Empowering a sustainable mobility furure with zero emission fuels from renewable electricity - Kraftstoffstudie II - Final Report.* 2016
41. Saba, S. M., Müller, M., Robinius, M., and Stolten, D., *The investment costs of electrolysis – A comparison of cost studies from the past 30 years.* International Journal of Hydrogen Energy, 2018. **43**(3): p. 1209-1223 DOI: 10.1016/j.ijhydene.2017.11.115.
42. Carmo, M., Fritz, D. L., Mergel, J., and Stolten, D., *A comprehensive review on PEM water electrolysis.* International Journal of Hydrogen Energy, 2013. **38**(12): p. 4901-4934 DOI: 10.1016/j.ijhydene.2013.01.151.
43. Müller-Langer, F., Majer, S., and O'Keeffe, S., *Benchmarking biofuels—a comparison of technical, economic and environmental indicators.* Energy, Sustainability and Society, 2014. **4**(1): p. 20 DOI: 10.1186/s13705-014-0020-x.

44. Robinius, M., Kuckertz, P., Stolten, D., Grube, T., Syranidis, K., Reuß, M., Stenzel, P., and Linßen, J., *Comparative Analysis of Infrastructures: Hydrogen Fueling and Electric Charging of Vehicles*. 2018, Elektrochemische Verfahrenstechnik
45. Kurzweil, P., and Dietlmeier, O. K., *Elektrochemische Speicher: Superkondensatoren, Batterien, Elektrolyse-Wasserstoff, rechtliche Grundlagen*. 2015, Wiesbaden: Springer Vieweg. 579 DOI: 10.1007/978-3-658-10900-4.
46. Edwards, R., Hass, H., Larivé, J.-F., Lonza, L., Maas, H., and Rickeard, D., *JRC Technical Reports - JEC Well-to-Wheels Analysis of Future Automotive Fuels and Powertrains in the European Context (JRC, EUCAR, CONCAWE).* 2014
47. Schiebahn, S., Grube, T., Robinius, M., Tietze, V., Kumar, B., and Stolten, D., *Power to gas: Technological overview, systems analysis and economic assessment for a case study in Germany.* International Journal of Hydrogen Energy, 2015. **40**(12): p. 4285–4294 DOI: 10.1016/j.ijhydene.2015.01.123.
48. Ho, M. T., and Wiley, D. E., *28 - Liquid absorbent-based post-combustion CO2 capture in industrial processes A2 - Feron, Paul H.M*, in *Absorption-Based Post-combustion Capture of Carbon Dioxide*. 2016, Woodhead Publishing. p. 711-756 DOI: doi.org/10.1016/B978-0-08-100514-9.00028-7.
49. Noothout, P., Wiersma, F., Hurtado, O., Macdonald, D., Kemper, J., and van Alphen, K., *CO2 Pipeline Infrastructure – Lessons Learnt.* Energy Procedia, 2014. **63**: p. 2481-2492 DOI: doi.org/10.1016/j.egypro.2014.11.271.
50. Smolinka, T., Günther, M., and Garche, J., *NOW-Studie "Stand und Entwicklungspotenzial der Wasserelektrolyse zur Herstellung von Wasserstoff aus regenerativen Energien"*. 2011
51. Mergel, J., Carmo, M., and Fritz, D., *Status on Technologies for Hydrogen Production by Water Electrolysis*, in *Transition to Renewable Energy Systems*. 2013, Wiley-VCH Verlag GmbH & Co. KGaA. p. 423-450 DOI: 10.1002/9783527673872.ch22.
52. Woods, D. R., *Rules of Thumb in Engineering Practice*. 2007. 1-44
53. Hirschberg, H. G., *Handbuch Verfahrenstechnik und Anlagenbau: Chemie, Technik und Wirtschaftlichkeit*. 2013: Springer Berlin Heidelberg
54. Rieckmann, T., *Persönliche Mitteilung*. 2017: Fortbildung Kostenschätzung, DECHEMA, Frankfurt
55. Schwencke, T., *BDEW-Strompreisanalyse Mai 2016 - Haushalte und Industrie*. 2017, BDEW Bundesverband der Energie- und Wasserwirtschaft e.V.: Berlin
56. Buddenberg, T., Bergins, C., and Harp, G., *Production of methanol from industry process gases.* Stahl und Eisen, 2016. **136**(6): p. 61-66
57. Tran, K.-C., Harp, G., Sigurbjornsson, O., Bergins, C., and Buddenberg, T., *Carbon Recycling for Converting Coke Oven Gas to Methanol for the Reduction of Carbon Dioxide at Steel Mills.*
58. Detz, R. J., Reek, J. N. H., and van der Zwaan, B. C. C., *The future of solar fuels: when could they become competitive?* Energy & Environmental Science, 2018 DOI: 10.1039/c8ee00111a.
59. Statista. *Jährliche Entwicklung des Wechselkurses des Euro gegenüber dem US-Dollar von 1999 bis 2017*. 2017 [Zugriff am 12.01.2018; Verfügbar über: https://de.statista.com/statistik/daten/studie/200194/umfrage/wechselkurs-des-euro-gegenueber-dem-us-dollar-seit-2001/.
60. JEC, *WELL-TO-TANK Appendix 1 - Version 4a (Conversion factors and fuel properties)*. 2014 DOI: 10.2790/95629
61. BASF SE. *Produzieren im Verbund*. 2017 [Zugriff am 24. September 2017]; Verfügbar über: https://www.basf.com/de/de/company/about-us/sites/ludwigshafen/production/the-production-verbund.html.
62. König, D. H., Freiberg, M., Dietrich, R.-U., and Wörner, A., *Techno-economic study of the storage of fluctuating renewable energy in liquid hydrocarbons.* Fuel, 2015. **159**: p. 289–297 DOI: 10.1016/j.fuel.2015.06.085.

63. Tremel, A., *Electricity-based fuels*. Springer briefs in applied sciences and technology. 2018, Cham: Springer. 95
64. Becker, W. L., Braun, R. J., Penev, M., and Melaina, M., *Production of Fischer–Tropsch liquid fuels from high temperature solid oxide co-electrolysis units.* Energy, 2012. **47**(1): p. 99–115 DOI: 10.1016/j.energy.2012.08.047.
65. Kohl, T., Laukkanen, T., Tuomaala, M., Niskanen, T., Siitonen, S., Järvinen, M. P., and Ahtila, P., *Comparison of energy efficiency assessment methods: Case Bio-SNG process.* Energy, 2014. **74**(Supplement C): p. 88-98 DOI: 10.1016/j.energy.2014.03.107.
66. Aspen Technology, I., *Aspen Plus®, Aspen Plus databanks, Version 8.8.*
67. Peters, M. S., Timmerhaus, K., and West, R., *Plant design and economics for chemical engineers*, ed. Edition, F. 2003: McGraw-Hill New York
68. Turton, R., Bailie, R. C., Whiting, W. B., and Shaeiwitz, J. A., *Analysis, Synthesis and Design of Chemical Processes (3rd Edition)*. 3rd ed. 2008: Pearson Education. 1088
69. Ulrich, G. D., *A guide to chemical engineering process design and economics*. 1984: Wiley New York
70. Alkhayat, W. A., and Gerrard, A. M., *Estimating Manning Levels for Process Plants.* AACE Transactions, I.2.1-I.2.4, 1984
71. Christensen, P., Dysert, L. R., Bates, J., Burton, D., Creese, R., and Hollmann, J., *Cost Estimate Classification system-as applied in engineering, procurement, and construction for the process industries.* AACE, Inc, 2005. **2011**
72. Otto, A., *Chemische, verfahrenstechnische und ökonomische Bewertung von Kohlendioxid als Rohstoff in der chemischen Industrie*. Schriftenreihe des Forschungszentrums Jülich : Reihe Energie & Umwelt. 2015, Jülich: Forschungszentrum Jülich. VIII, 272 S
73. Hansen, J. B., and Højlund Nielsen, P. E., *Methanol Synthesis*, in *Handbook of Heterogeneous Catalysis*. 2008, Wiley-VCH: Weinheim. p. 2920-2949 DOI: 10.1002/9783527610044.hetcat0148.
74. Pérez-Fortes, M., Schöneberger, J. C., Boulamanti, A., and Tzimas, E., *Methanol synthesis using captured CO2 as raw material: Techno-economic and environmental assessment.* Applied Energy, 2016. **161**: p. 718–732 DOI: 10.1016/j.apenergy.2015.07.067.
75. Al-Kalbani, H., Xuan, J., García, S., and Wang, H., *Comparative energetic assessment of methanol production from CO2: Chemical versus electrochemical process.* Applied Energy, 2016. **165**: p. 1-13 DOI: 10.1016/j.apenergy.2015.12.027.
76. Van-Dal, É. S., and Bouallou, C., *Design and simulation of a methanol production plant from CO2 hydrogenation.* Journal of Cleaner Production, 2013. **57**: p. 38-45 DOI: doi.org/10.1016/j.jclepro.2013.06.008.
77. Engineering, I. S. a. *DME production process flow sheet*. 2012 [Zugriff am 22. April 2018]; Verfügbar über: http://www.inclusive-science-engineering.com/dme/.
78. Müller, M., and Hübsch, U., *Dimethyl Ether*, in *Ullmann's Encyclopedia of Industrial Chemistry*. 2000, Wiley-VCH Verlag GmbH & Co. KGaA DOI: 10.1002/14356007.a08_541.
79. Lu, P., Yang, G., Tanaka, Y., and Tsubaki, N., *Ethanol direct synthesis from dimethyl ether and syngas on the combination of noble metal impregnated zeolite with Cu/ZnO catalyst.* Catalysis Today, 2014. **232**: p. 22-26 DOI: 10.1016/j.cattod.2013.10.042.
80. Yang, G., San, X., Jiang, N., Tanaka, Y., Li, X., Jin, Q., Tao, K., Meng, F., and Tsubaki, N., *A new method of ethanol synthesis from dimethyl ether and syngas in a sequential dual bed reactor with the modified zeolite and Cu/ZnO catalysts.* Catalysis Today, 2011. **164**(1): p. 425-428 DOI: 10.1016/j.cattod.2010.10.027.
81. Pavlíček, J., Bogdanić, G., and Wichterle, I., *Vapour–liquid and chemical equilibria in the ethyl ethanoate+ethanol+propyl ethanoate+propanol system accompanied with transesterification reaction.* Fluid Phase Equilibria, 2012. **328**: p. 61-68 DOI: doi.org/10.1016/j.fluid.2012.05.016.

82. Riittonen, T., Salmi, T., Mikkola, J.-P., and Wärnå, J., *Direct Synthesis of 1-Butanol from Ethanol in a Plug Flow Reactor: Reactor and Reaction Kinetics Modeling.* Topics in Catalysis, 2014. **57**(17): p. 1425-1429 DOI: 10.1007/s11244-014-0314-4.
83. *Sicherheitsdatenblatt 1-Butanol*, KG, C. R. G. C., Editor. 2015
84. Khan, Y., Marin, M., Karinen, R., Lehtonen, J., and Kanervo, J., *1-Butanol dehydration in microchannel reactor: Kinetics and reactor modeling.* Chemical Engineering Science, 2015. **137**: p. 740-751 DOI: 10.1016/j.ces.2015.07.026.
85. Kropf, H., *Alkohole als Petrochemikalien.* Chemie Ingenieur Technik, 1966. **38**(8)
86. Patankar, S. C., and Yadav, G. D., *Cascade engineered synthesis of 2-ethyl-1-hexanol from n-butanal and 2-methyl-1-pentanol from n-propanal using combustion synthesized Cu/Mg/Al mixed metal oxide trifunctional catalyst.* Catalysis Today, 2017 DOI: 10.1016/j.cattod.2017.01.008.
87. Raizada, V. K., Tripathi, V. S., Lal, D., Singh, G. S., Dwivedi, C. D., and Sen, A. K., *Kinetic Studies on Dehydrogenation of Butanol to Butyraldehyde Using Zinc Oxide as Catalyst.* J. Chem. Tech. Biotechnol., 1993. **56**: p. 265-270
88. Reuss, G., Disteldorf, W., Gamer, A. O., and Hilt, A., *Formaldehyde*, in *Ullmann's Encyclopedia of Industrial Chemistry, Vol. 15*. 2012, Wiley-VCH Verlag GmbH & Co. KGaA DOI: 10.1002/14356007.a11_619.
89. Chauvel, A., and Lefebvre, G., *Petrochemical Processes*. Editions OPHRYS
90. Maurer, G., *Vapor-Liquid Equilibrium of Formaldehyde- and Water-Containing Multicomponent Mixtures.* AIChE Journal, 1986. **32**(6): p. 932-948
91. Albert, M., Hahnenstein, I., Hasse, H., and Maurer, G., *Vapor−Liquid and Liquid−Liquid Equilibria in Binary and Ternary Mixtures of Water, Methanol, and Methylal.* Journal of Chemical & Engineering Data, 2001. **46**(4): p. 897-903 DOI: 10.1021/je000352l.
92. Panzer, E., and Emig, G., *Verfahrensoptimierung der technischen Formaldehydsynthese am Silberkatalysator*, in *FORKAT II, Teilprojekt C.6*. 2000, Lehrstuhl für Technische Chemie I, Universität Erlangen-Nürnberg
93. Grützner, T., *Entwicklung eines destillationsbasierten Verfahrens zur Herstellung von Trioxan*. 2007, Institut für Technische Thermodynamik und Thermische Verfahrenstechnik, Universität Stuttgart. p. 250
94. Grützner, T., Hasse, H., Lang, N., Siegert, M., and Ströfer, E., *Development of a new industrial process for trioxane production.* Chemical Engineering Science, 2007. **62**(18–20): p. 5613-5620 DOI: 10.1016/j.ces.2007.01.047.
95. Friese, T., Hasse, H., Lang, N., Siegert, M., Stammer, A., and Stroefer, E., *Verfahren zur Abtrennung von Trioxan aus einem Trioxan/Formaldehyd/Wasser-Gemisch mittels Druckwechsel-Rektifikation* 2005
96. Hasse, H., Drunsel, J.-O., Burger, J., Schmidt, U., Renner, M., and Blagov, S., *Process for the Production of pure Methylal*. 2014: USA. p. 8
97. Drunsel, J.-O., *Entwicklung von Verfahren zur Herstellung von Methylal und Ethylal*, in *Scientific report series / Laboratory of Engineering Thermodynamics*. 2012, Techn. Univ: Kaiserslautern. p. 162
98. Schmitz, N., Strofer, E., Burger, J., and Hasse, H., *Conceptual Design of a Novel Process for the Production of Poly(oxymethylene) Dimethyl Ethers from Formaldehyde and Methanol.* Industrial & Engineering Chemistry Research, 2017. **56**(40): p. 11519-11530 DOI: 10.1021/acs.iecr.7b02314.
99. Burger, J., Schmitz, N., Hasse, H., and Stroefer, E., *Process for preparing polyoxymethylene dimethyl ethers from formaldehyde and methanol in aqueous solutions*. 2018: United States
100. Oestreich, D., Lautenschütz, L., Arnold, U., and Sauer, J., *Reaction kinetics and equilibrium parameters for the production of oxymethylene dimethyl ethers (OME) from methanol and*

formaldehyde. Chemical Engineering Science, 2017. **163**(Supplement C): p. 92-104 DOI: 10.1016/j.ces.2016.12.037.

101. Burger, J., Ströfer, E., and Hasse, H., *Production process for diesel fuel components poly(oxymethylene) dimethyl ethers from methane-based products by hierarchical optimization with varying model depth.* Chemical Engineering Research and Design, 2013. **91**(12): p. 2648-2662 DOI: doi.org/10.1016/j.cherd.2013.05.023.
102. Haltenort, P., Hackbarth, K., Oestreich, D., Lautenschütz, L., Arnold, U., and Sauer, J., *Heterogeneously catalyzed synthesis of oxymethylene dimethyl ethers (OME) from dimethyl ether and trioxane.* Catalysis Communications, 2018. **109**: p. 80-84
103. Keil, F. J., *Methanol-to-hydrocarbons: process technology.* Microporous and Mesoporous Materials, 1999. **29**(1): p. 49-66 DOI: 10.1016/S1387-1811(98)00320-5.
104. Phillips, S. D., Tarud, J. K., Biddy, M. J., and Dutta, A., *Gasoline from Wood via Integrated Gasification, Synthesis, and Methanol-to-Gasoline Technologies*. 2011, NREL - National Renewable Energy Laboratory: Golden, Colorado. p. 115
105. de Klerk, A., *Fischer-Tropsch fuels refinery design.* Energy and Environmental Science, 2011. **4**(4): p. 1177-1205 DOI: 10.1039/c0ee00692k.
106. de Klerk, A., *Can Fischer-Tropsch syncrude be refined to on-specification diesel fuel?* Energy and Fuels, 2009. **23**(9): p. 4593-4604 DOI: 10.1021/ef9005884.
107. Dry, M. E., *High quality diesel via the Fischer-Tropsch process - A review.* Journal of Chemical Technology and Biotechnology, 2002. **77**(1): p. 43-50 DOI: 10.1002/jctb.527.
108. de Klerk, A., *Fischer-Tropsch Refining*, in *Department of Chemical Engineering*. 2008, University of Pretoria DOI: 10.1002/9783527635603.
109. Dry, M., and Steynberg, A., *Fischer-Tropsch Technology, Volume 152*. 1 ed. 2004: Elsevier Science. 722
110. Vervloet, D., Kapteijn, F., Nijenhuis, J., and van Ommen, J. R., *Fischer-Tropsch reaction-diffusion in a cobalt catalyst particle: aspects of activity and selectivity for a variable chain growth probability.* Catalysis Science & Technology, 2012. **2**(6): p. 1221-1233 DOI: 10.1039/C2CY20060K.
111. Kaiser, P., Unde, R. B., Kern, C., and Jess, A., *Production of Liquid Hydrocarbons with CO 2 as Carbon Source based on Reverse Water-Gas Shift and Fischer-Tropsch Synthesis.* Chemie Ingenieur Technik, 2013. **85**(4): p. 489–499 DOI: 10.1002/cite.201200179.
112. Verdegaal, W. M., Becker, S., and Olshausen, C. V., *Power-to-liquids: Synthetic crude oil from CO2, water, and sunshine.* Chemie-Ingenieur-Technik, 2015. **87**(4): p. 340-346 DOI: 10.1002/cite.201400098.
113. Machhammer, O., Bode, A., and Hormuth, W., *Financial and Ecological Evaluation of Hydrogen Production Processes on Large Scale.* Chemie Ingenieur Technik, 2015. **87**(4): p. 409-418 DOI: 10.1002/cite.201400151.

Appendix

Table A1. Educt demand of fuel syntheses based on H_2 and CO_2.

Product	kg_{H2}/kg_{Fuel}	kg_{H2}/l_{DE}	kg_{CO2}/kg_{Fuel}	kg_{CO2}/l_{DE}	MJ_{Steam}/kg_{CO2}
Hydrogen	1	0.299	-	-	-
Methanol	0.189	0.340	1.373	2.476	1.21 (175 °C) + 0.07 (125 °C)
Ethanol	0.283	0.380	1.872	2.511	0.99 (175 °C) + 0.39 (125 °C)
1-Butanol	0.383	0.416	2.316	2.512	1.23 (175 °C) + 0.71 (125 °C)
2-Butanol	0.391	0.425	2.316	2.519	1.62 (175 °C) + 0.78 (125 °C)
iso-Octanol	0.446	0.426	2.637	2.520	0.45 (175 °C) + 1.23 (125 °C)
DME	0.263	0.327	1.911	2.379	0.04 (175 °C) + 0.37 (125 °C)
OME_1	0.270	0.410	1.968	2.987	0
OME_{3-5} A	0.268	0.500	1.949	3.640	1.30 (175 °C) + 0.34 (125 °C)
OME_{3-5} B	0.269	0.505	1.961	3.673	0
OME_{3-5} C	0.267	0.500	1.941	3.637	0
MTG	0.403	0.333	2.874	2.373	0.85 (250 °C) + 1.346 (175 °C) + 0.11 (125 °C)
FT	0.480	0.391	3.056	2.494	4.66 (175 °C) + 1.91 (125 °C)

Table A2. Technology readiness level and efficiencies of fuel synthesis based on H_2 and CO_2.

Product of synthesis route	TRL	Chemical conversion η_{LHV} (Eq. 2)	$\eta_{LHV,max}$ (Eq. 2)	Plant efficiency η_P (Eq.3)	Efficiency factor f (Eq. 4)	Power-to-Fuel efficiency η_{PTL} (Eq. 5)
Hydrogen	-	1	1	-	-	0,7
Methanol	9	0.880	0.880	0.859	0.976	0.576
Ethanol	4	0.788	0.851	0.744	0.944	0.507
1-Butanol	4	0.720	0.834	0.662	0.920	0.457
2-Butanol	4	0.704	0.831	0.612	0.869	0.438
iso-Octanol	4	0.702	0.843	0.593	0.845	0.420
DME	9	0.916	0.916	0.894	0.976	0.600
OME_1	5	0.729	0.827	0.643	0.882	0.448
OME_{3-5} A	4	0.598	0.736	0.409	0.684	0.305
OME_{3-5} B	4	0.593	0.725	0.379	0.639	0.288
OME_{3-5} C	4	0.599	0.715	0.354	0.591	0.274
MTG	9	0.899	-	0.875	0.973	0.589
FT *($C_{16}H_{34}$)*	6	0.765	*(0.840)*	0.749	0.981	0.506

A plausibility test regarding the efficiencies shown in

Table A2 is given in the Supplementary Material.

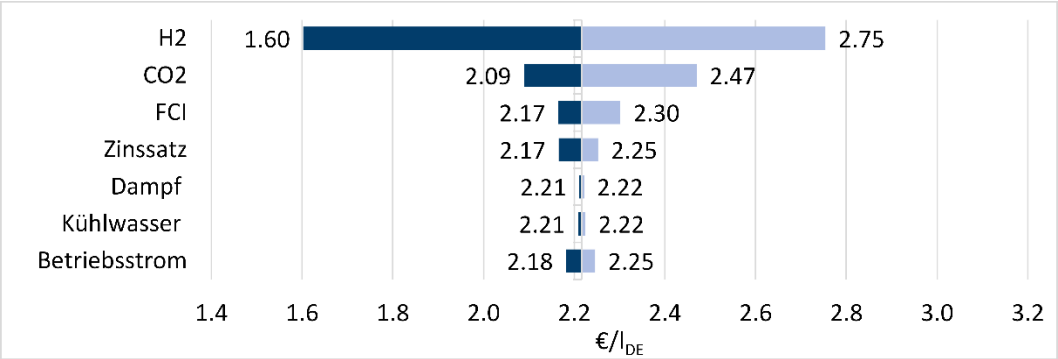

Figure A1. Sensitivity analysis regarding the synthesis costs of ethanol from H_2 and CO_2.

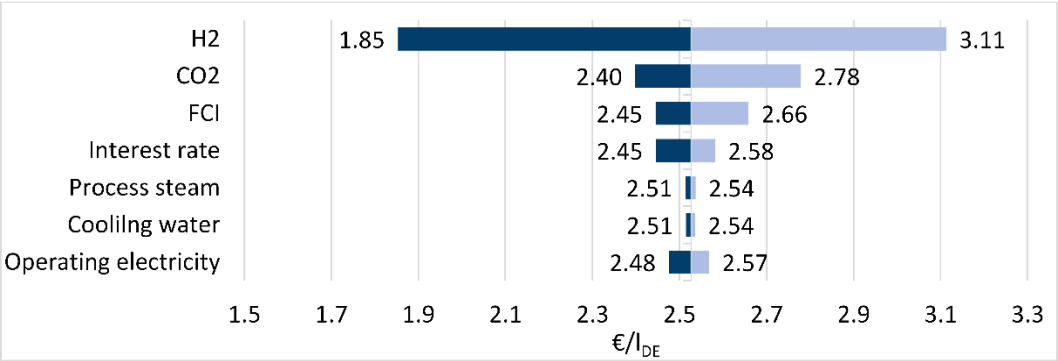

Figure A2. Sensitivity analysis regarding the synthesis costs of 1-butanol from H_2 and CO_2.

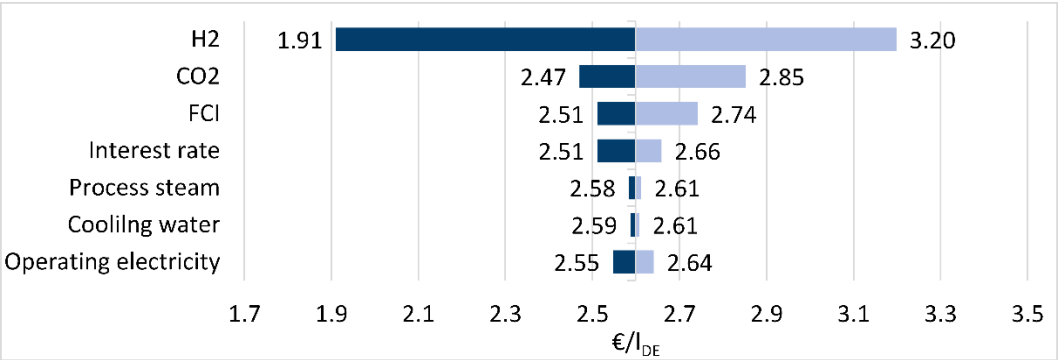

Figure A3. Sensitivity analysis regarding the synthesis costs of 2-butanol from H_2 and CO_2.

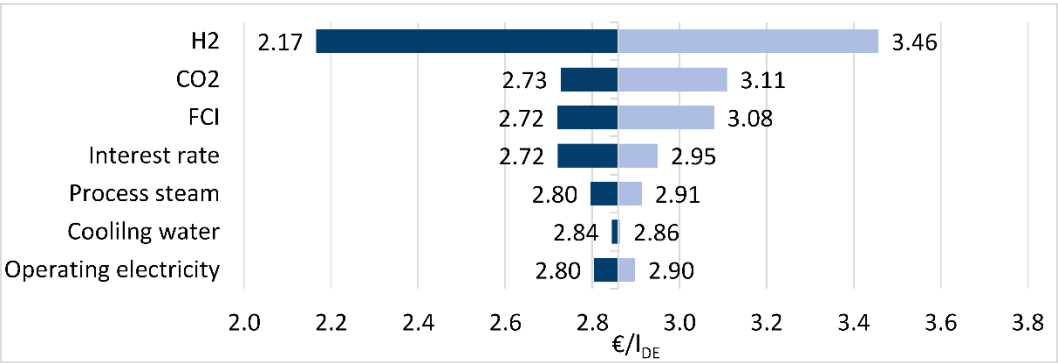

Figure A4. Sensitivity analysis regarding the synthesis costs of iso-octanol from H_2 and CO_2.

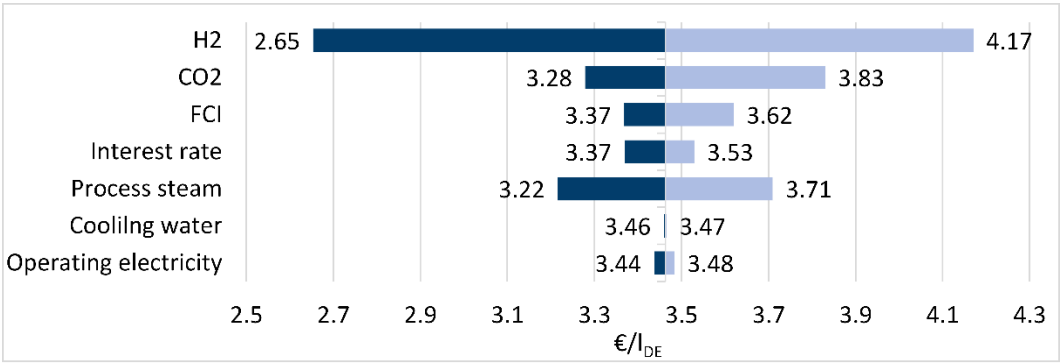

Figure A5. Sensitivity analysis regarding the synthesis costs of OME_{3-5} via route A from H_2 and CO_2.

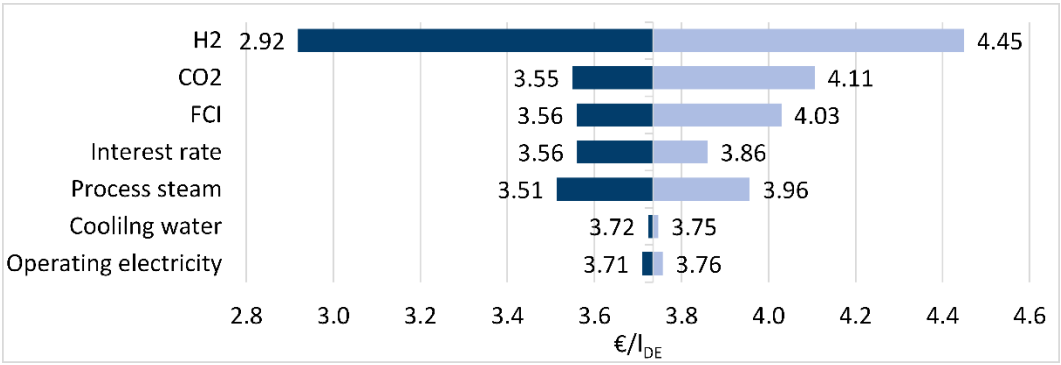

Figure A6. Sensitivity analysis regarding the synthesis costs of OME_{3-5} via route B from H_2 and CO_2.

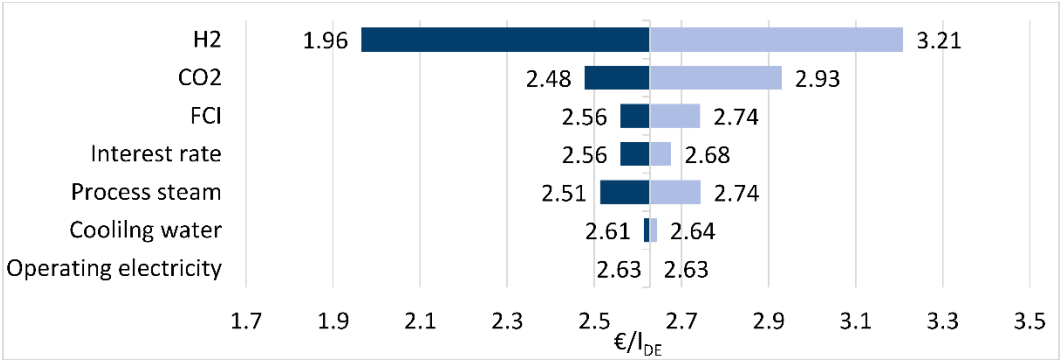

Figure A7. Sensitivity analysis regarding the synthesis costs of OME_1 from H_2 and CO_2.

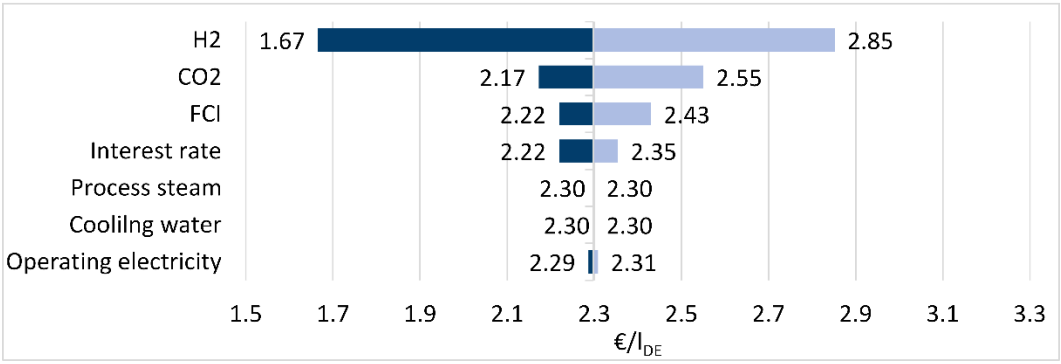

Figure A8. Sensitivity analysis regarding the synthesis costs of hydrocarbons from H_2 and CO_2 via Fischer-Tropsch.

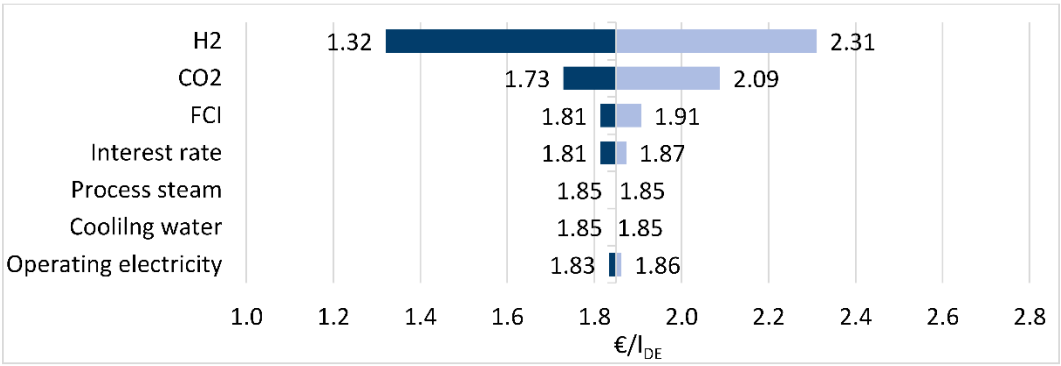

Figure A9. Sensitivity analysis regarding the synthesis costs of DME from H_2 and CO_2.

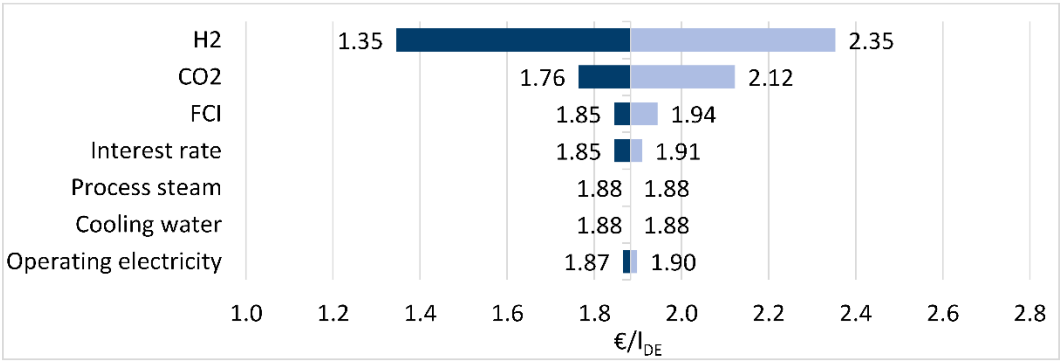

Figure A10. Sensitivity analysis regarding the synthesis costs of hydrocarbons from H_2 and CO_2 via MTG.